

# Connecting quantum circuit amplitudes and matrix permanents through polynomials

Hugo Thomas, Pierre-Emmanuel Emeriau, and Rawad Mezher

Quandela SAS, 7 Rue Léonard de Vinci, 91300 Massy, France

In this paper, we strengthen the connection between qubit-based quantum circuits and photonic quantum computation. Within the framework of circuit-based quantum computation, the sum-over-paths interpretation of quantum probability amplitudes leads to the emergence of sums of exponentiated polynomials. In contrast, the matrix permanent is a combinatorial object that plays a crucial role in photonic by describing the probability amplitudes of linear optical computations. To connect the two, we introduce a general method to encode an  $\mathbb{F}_2$ -valued polynomial with complex coefficients into a graph, such that the permanent of the resulting graph's adjacency matrix corresponds directly to the amplitude associated the polynomial in the sum-over-path framework. This connection allows one to express quantum amplitudes arising from qubit-based circuits as permanents, which can naturally be estimated on a photonic quantum device.

## 1 Introduction

Quantum computation is often pictured in the gate-based model where computations are described by quantum logic gates. Quantum computing (QC) based on qubits is predominant as its development has mirrored that of classical computer science, which relies on bits as the information carrier.

Photonic quantum computing is a different yet promising avenue for realising a quantum computer [1, 2], since photonic approaches are modular and flexible, and that photons hardly suffer from decoherence. Photonic QC is not naturally described by qubit logic, though. Rather, Aaronson and Arkhipov [3] showed that output probability amplitudes of photons in a linear optical interferometer (BosonSampling) can be expressed as permanents of sub-matrices of the linear interferometer. More precisely, the quantum probability amplitudes resulting from a linear optical computation on  $m$  modes are – for input and output occupancy  $\mathbf{s} = (s_1, \dots, s_m)$  and  $\mathbf{t} = (t_1, \dots, t_m)$ , where  $s_i$  (resp.  $t_i$ ) is the number of photons in input (resp.

output) mode  $i$ , and a unitary matrix  $\mathcal{U} \in SU(m)$  – of the form

$$\langle \mathbf{t} | \mathcal{U} | \mathbf{u} \rangle \propto \text{Per}(\mathcal{U}_{\mathbf{s}, \mathbf{t}}). \quad (1)$$

Computing the matrix permanent is in all generality a so-called #P-hard problem – that is, a problem that amounts to counting the number of solutions to an NP-hard problem; in [4] it is shown that it is a #P-complete problem for binary matrices.

Sums of exponentiated polynomials<sup>1</sup> appear in many domains ranging from number theory [7, 8] and computational complexity theory [9] to Feynman's interpretation of quantum mechanics [10]. In [11], the authors relied on a discretised version of Feynman's path-integral formulation to show that computing quantum circuits probability amplitudes is equivalent to compute such sums. More precisely, given a quantum circuit  $\mathcal{C}$  acting on  $n$  qubits, the probability amplitude of a given input-output pair  $\mathbf{a}, \mathbf{b} \in \{0, 1\}^n$  is given by the sum

$$\langle \mathbf{b} | \mathcal{C} | \mathbf{a} \rangle \propto \sum_{\mathbf{x} \in \{0, 1\}^v} e^{if(\mathbf{x})}, \quad (2)$$

where  $f$  is an  $\mathbb{F}_2$ -valued polynomial with complex coefficients and  $v$  is the number of qubits in the circuit plus the number of gates creating coherence in the circuit (*e.g.*, Hadamard gates). From this result follows that computing quantum circuits probability amplitudes is also a #P-hard function [12].

Intrigued by the suggestion at the end of [13] regarding the potential estimation of quantum circuits amplitude via classical techniques coming from the linear optical picture [14, 15], we aim to derive a formal mapping between gate-based computation and linear optical computation for amplitude estimation. The two seemingly different models of computation yields quantum probability amplitudes the computation of which lie in the same complexity class. This raises the question of the precise relationship between these two models.

**Our contributions.** From a  $n$ -variable polynomial  $f$  with binary variables and complex coefficients, we show how to construct a graph  $G$  with adjacency ma-

Hugo Thomas: [hugo.thomas@quandela.com](mailto:hugo.thomas@quandela.com)

<sup>1</sup>Also called *exponential sums* in [5, 6].

trix  $\mathcal{G}$  such that

$$\sum_{\mathbf{x} \in \{0,1\}^n} e^{if(\mathbf{x})} = \text{Per}(\mathcal{G}), \quad (3)$$

in time polynomial in the number of clauses of  $f$ . That is to say, the permanent computes the sum of the exponential of a polynomial  $f$  evaluated over all its domain. We go beyond already existing techniques [4, 13, 16] by providing a systematic recipe for constructing such a graph. To do so, each clause of the polynomial is encoded onto a small graph, called a *clause-gadget*, according to its degree. For a fixed degree, the graph gadget is parameterized by the clause coefficient. While we find that designing a graph gadget is a computationally hard problem<sup>2</sup>, we perform the computation for clauses of degree up to 3 in Section 3.2. This encoding finds uses in quantum circuits probability amplitude computation. It was shown in [17] that it is possible to encode the adjacency matrix of a graph  $G(V, E)$  onto a unitary matrix  $\mathcal{U}$  such that

$$\langle \mathbf{1}_n | \mathcal{U} | \mathbf{1}_n \rangle \propto \text{Per}(\mathcal{G}),$$

where  $|\mathbf{1}_n\rangle = |1^{\otimes n} 0^{\otimes m-n}\rangle$ . Thus, given the graph  $G_{\mathcal{C}}(V, E)$  encoding the amplitude  $\langle \mathbf{b} | \mathcal{C} | \mathbf{a} \rangle$  of a quantum circuit  $\mathcal{C}$ , for  $\mathbf{a}, \mathbf{b} \in \{0, 1\}^n$ , our encoding allows one to construct a linear optical circuit  $\mathcal{V}$  such that

$$\langle \mathbf{1}_n | \mathcal{V} | \mathbf{1}_n \rangle \propto \langle \mathbf{b} | \mathcal{C} | \mathbf{a} \rangle.$$

While Rudolph’s encoding [13] focuses on a particular gate set and does not provide a generic recipe for designing suitable gadgets, we formalize the encoding and provide a systematic recipe for constructing such gadgets. We do so by deriving a procedure that checks the existence of a gadget and guarantees its construction in Theorem 1. We discuss potential applications of our encoding in Section 4.

## 2 Overview of the framework

Foremost, we start with a brief overview of the framework. We recall in Appendix A the linear algebraic tools used throughout this work.

In [13], the author shows how to encode a family of specific polynomials that encode an amplitude of a quantum circuit onto a graph, such that the permanent of the adjacency matrix of the graph equals the amplitude. The technique relies on a seminal work from Valiant [4], where such a graph encoding is used to show that computing the permanent of a binary matrix is a  $\#\text{P}$ -complete problem. Formally, in linear algebra, the permanent of a square matrix  $A = (a_{i,j})_{0 \leq i,j \leq n}$  of order  $n$ , which we write  $\text{Per}(A)$ , is defined as the following function of its entries [18]:

$$\text{Per}(A) = \sum_{\sigma \in S_n} \prod_{i=1}^n a_{i,\sigma(i)}, \quad (4)$$

<sup>2</sup>Although note that it is a compute once and store forever problem.

where the sum extends over all elements of the symmetric group  $S_n$ . Despite its apparent similarities with the determinant, the essence of the permanent is counting and it has, unlike the determinant, no known geometrical interpretation. From a graph-theoretic point of view, the permanent of the adjacency matrix of a directed graph – *i.e.*, the direction of the edges matters – is equal to the sum of the weights of all *cycle covers* of the graph (defined shortly after). Aaronson proved that computing the permanent is  $\#\text{P}$ -hard in the general case using linear optics techniques [19].

We use the notation  $G(V, E)$  to denote a graph with vertex set  $V$ , and edge set  $E$ , or  $G$  for simplicity if these sets are irrelevant, and we denote its adjacency matrix by  $\mathcal{G}$ , *i.e.*, the same symbol with calligraphic font.

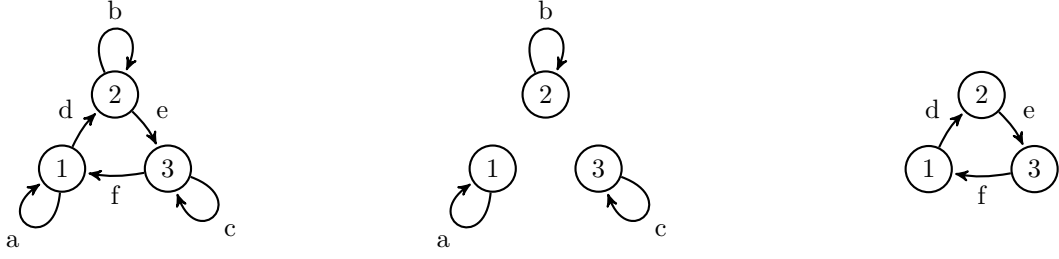
We consider hereafter directed and weighted graphs. In such a graph, a *cycle* is a closed path. A *cycle cover* is a set of vertex-disjoint cycles that covers *all* vertices, *i.e.*, no vertex is left alone. In all generality, a graph admits several cycle covers and given one of them, its weight is the product of the weights of the edges involved in that particular cover. We show examples of graph cycle covers in Figure 1.

Providing a graph  $G(V, E)$  satisfying Equation (3) is achieved by encoding each monomial (also identified as clauses) of the polynomial  $f$  onto a small graph, the so-called *clause gadgets*, and those gadgets are linked together with cycles representing the variables they share to form the graph. From the perspective of the graph, the permanent of its adjacency matrix equals the sum of the weights of all its cycle covers. The permanent of the graph relates to evaluating the polynomial as follows. In a particular cycle cover, the absence of a cycle corresponding to a variable corresponds to the fact that the variable is assigned the value 1, and its presence corresponds to its assignment to 0. We hereafter use the following coloring convention: the blue cycles encode the variables while linear, quadratic and cubic clauses are respectively represented by red, green and purple graph-gadgets.

For the sake of completeness, we first explain how exponential sums may appear in quantum computation. In [11] a method – known as the *sum-over-paths* formalism – is given to encode the quantum amplitudes of {Hadamard, Toffoli} circuits as the gap of a low-degree polynomial over  $\mathbb{F}_2$ . Precisely, for a  $q$ -qubit circuit  $\mathcal{C}$  comprising  $h$  Hadamard gates, it is shown how to construct a polynomial  $f \in \mathbb{F}_2[x_1, \dots, x_n]$  with  $n = q + h$  variables such that

$$\langle \mathbf{b} | \mathcal{C} | \mathbf{a} \rangle = \sum_{\mathbf{x} \in \{0,1\}^n} \frac{(-1)^{f(\mathbf{x})}}{\sqrt{2}^h}, \quad (5)$$

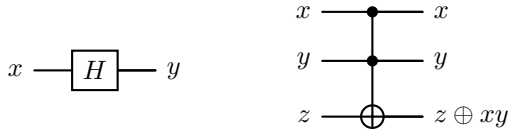
where  $|\mathbf{a}\rangle$  and  $|\mathbf{b}\rangle$  are arbitrary input and output states, by applying the following procedure. In the rest, we will refer to  $\langle \mathbf{b} | \mathcal{C} | \mathbf{a} \rangle$  as the *amplitude of interest* with the multiset notation  $\mathbf{x} = (x_1, \dots, x_n)$ ,



(a) A 3-vertex graph denoted  $G$ . (b) A cycle cover of  $G$  of weight  $abc$ . (c) Another cycle cover of  $G$  of weight  $def$ .

Figure 1: The leftmost graph of Figure 1a is a graph with 3 vertices. The two graphs depicted in Figures 1b and 1c are the two cycle covers graph of Figure 1a – so that if  $G$  denotes the leftmost graph,  $\text{Per}(G) = abc + def$ .

and consider the  $a_i$ 's and  $b_j$ 's as input and output variables respectively. The  $a_i$ 's travel along their respective qubit line. Whenever a variable  $x$  goes through a Hadamard gate, a new one is created (Figure 2a), while when a variable  $z$  traverses the target of a Toffoli gate, no variable is created but it is replaced by  $z \oplus xy$  where  $x, y$  are the variables living on the two control lines that remain unchanged (Figure 2b). The output bit values  $B_j(\mathbf{x})$  are polynomi-



(a) Hadamard gate. (b) Toffoli gate.

Figure 2: Rules to follow to act on the variables.

als over  $\mathbb{F}_2[x_1, \dots, x_n]$ , where  $n$  is the total number of path variables. Any assignment of  $\mathbf{x}$  is valid if it satisfies the condition  $B_j(\mathbf{x}) = b_j$  for all  $j$ , which we write  $\mathbf{B}(\mathbf{x}) = \mathbf{b}$ . Once all the path variables are created, the circuit is associated to the polynomial constructed by taking the sum over  $\mathbb{F}_2$  of the product of every pairs of variables on either side of a Hadamard gate, namely

$$f(\mathbf{x}) = \sum_{\text{Hadamard gates } h} (\text{input var. of } h)(\text{output var. of } h),$$

as this generalizes to all Hadamard gates the identity

$$\langle x|H|y \rangle = \frac{1}{\sqrt{2}} e^{i\pi xy}. \quad (6)$$

Taking the sum over all possible assignments of the variables gives the exponential sum of Equation (5). From this quantum amplitude encoding to polynomial, the contribution of [13] is a procedure to construct a graph  $G$  such that

$$\langle \mathbf{b}|\mathcal{C}|\mathbf{a} \rangle = \frac{\text{Per}(\mathcal{G})}{\sqrt{2}^h}, \quad (7)$$

for circuit  $\mathcal{C}$  built upon the same gate set. Denote by  $\mathcal{G}$  the circuit of Figure 3, the graph encoding of

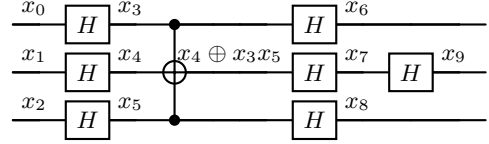


Figure 3: Instance of {Hadamard, Toffoli} circuit, with superimposed variables following the rules of Figure 2. The vector of variables is  $\mathbf{x} = (x_0, \dots, x_{12})$ . The input state is  $|\mathbf{a}\rangle = |x_0, x_1, x_2\rangle$  and the vector of conditions is  $\mathbf{B}(\mathbf{x}) = (x_6, x_9, x_8)^T$ . The polynomial associated to the circuit is  $f(\mathbf{x}) = x_0x_3 \oplus x_1x_4 \oplus x_2x_5 \oplus x_3x_6 \oplus x_4x_7 \oplus x_3x_5x_7 \oplus x_5x_8 \oplus x_7x_9$ . The pair of Hadamard gates that create the variables  $x_7$  and  $x_9$  amounts to the identity, but enforce the polynomial to have degree (at most) 3.

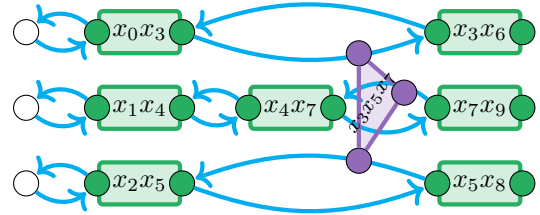


Figure 4: Graph corresponding to the circuit of Figure 3, encoding input and output states  $|000\rangle$  and  $|111\rangle$  respectively. Recall that the circuit was associated to the polynomial  $f(\mathbf{x}) = x_0x_3 \oplus x_1x_4 \oplus x_2x_5 \oplus x_3x_6 \oplus x_4x_7 \oplus x_3x_5x_7 \oplus x_5x_8 \oplus x_7x_9$ . The green squares (resp. red triangles) represent the quadratic (resp. cubic) clause gadgets. The blue cycles correspond to the variables. We denote by  $G$  the above graph and  $\mathcal{C}$  the circuit of Figure 3, then it holds that  $\langle 111|\mathcal{C}|000 \rangle = \frac{\text{Per}(\mathcal{G})}{8\sqrt{2}}$ .

$\langle 111|\mathcal{C}|000 \rangle$  is illustrated in Figure 4. This encoding, however, imposes strong constraints on the structure of the polynomial. Namely, the polynomial must be of degree at most 3, and the variables that appear in a cubic clause must appear in exactly two quadratic clauses. This constraint is satisfied by adding redundant pairs of Hadamard gate which, by construction, bound the degree of the polynomial. Hence, the proposal of [13] is tailored to encode the polynomials giving the quantum amplitudes of circuits built upon the Hadamard and Toffoli gates.

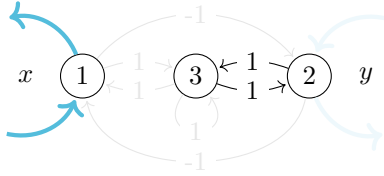


Figure 5: *Valid cycle cover* (**Observation 1**) of the gadget representing the quadratic clauses of the polynomial from [13]. Here is illustrated the gadget  $A_2(\pi)$  (see **Section 3.2**). Say vertex 1 is connected to the variable  $x$  and 2 to  $y$ , then the cycle cover assigns  $x = 0$  and  $y = 1$ , and the contribution of the gadget is  $(-1)^{xy} = 1$ .

In the next section, we describe how to construct suitable clause gadgets for polynomials without constraining their structure.

### 3 General method for deriving clause gadgets

We encode polynomials of the form

$$f(x_1, \dots, x_n) = \sum_{S \subseteq [n]} \theta_S \prod_{i \in S} x_i, \quad (8)$$

with boolean variables  $x_i$  and complex coefficients  $\theta_S$  onto graphs. To do so, each clause  $\theta_S \prod_{i \in S} x_i$  is associated to a graph-gadget, since using the identity

$$\sum_{\mathbf{x}} e^{i \sum_{S \subseteq [n]} \theta_S \prod_{i \in S} x_i} = \sum_{\mathbf{x}} \prod_{S \subseteq [n]} e^{i \theta_S \prod_{i \in S} x_i}, \quad (9)$$

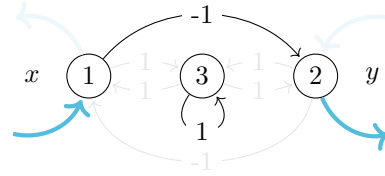
we find that we can treat each clause separately: observe that the left-hand side of **Equation (9)** has the same sum-of-products form as the permanent of **Equation (4)**.

First in [4], and later in [13], was shown that a gadget must satisfy the two following simple observations to be a valid one:

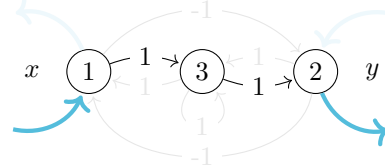
**Observation 1** (*nonzero contributions*). *If a cycle cover is consistent with an assignment of the variables, then the weight of that cycle cover must be the value of  $f$  evaluated for that assignment of the variables (see **Figure 5**).*

**Observation 2** (*zero contributions*). *The inconsistent cycle covers must have an overall weight of zero (see **Figure 6**).*

The clause gadget of a clause of degree  $d$  is a graph with at least  $d$  vertices, and the two above observations can be satisfied by adding a certain number of additional *inner* vertices if necessary. **Algorithm 1** describes the procedure to explicitly write down all the constraints a particular clause gadget must satisfy as a system of polynomial equations.



(a) Part of a crossing cycle.



(b) Part of another crossing cycle.

Figure 6: *Invalid cycle cover*: the cycles representing the variables are partially covered. The gadget design must be so that each crossing path can be paired with another with contribution of opposite sign to the cycle cover in a way which causes the necessary cancellation (**Observation 2**). In this instance, the contribution depicted in **Figure 6a** is cancelled by the one shown in **Figure 6b**.

Questions remain open: first and foremost, how do we find a solution to that system? What is the minimal size of the graph associated to a given clause? To answer these two questions, we extensively rely on Gröbner basis theory [20].

Designing clause gadgets involves solving a system of matrix permanents, whose size depends on the degree of the clause to be encoded. State-of-the-art algorithms for computing Gröbner bases, such as F5 [21], have exponential time complexity [22]. We believe that our method is the most efficient way to design a gadget, as we draw up the minimal set of constraints that a gadget must satisfy to be valid. Hence, we conjecture that designing a suitable clause gadget is a computationally hard problem, the requirement of computing permanents cannot be removed, as at least the permanent of the gadget must equal the encoded amplitude.

#### 3.1 Clause gadget design

This section is intended to explain how the methods of [4, 13, 16] can be formalized and how the finding of a clause-gadget can be systematized. The two **Observations 1** and **2** of **Section 3** are suitably described mathematically employing computational algebraic geometry techniques. Given a gadget, we denote by *outer vertices* all the vertices connected to the rest of the graph, *i.e.*, the vertices associated to the variables, and by *inner vertices* the vertices only connected within the gadget. The inner vertices will account for additional degrees of freedom in the weights the cycle covers of the gadget so that all the constraints (see the rest of the section) are satisfied. For instance, in **Figures 5** and **6**, the *outer vertices* are

the vertices 1 and 2, and the vertex 3 is the only *inner vertex*. We now describe how [Observations 1 and 2](#) translate into a system of equations, a solution of which is the gadget we seek. Say one wants to represent a clause of degree  $d$ , and requires  $k$  inner degrees of freedom, *i.e.*,  $k$  additional inner vertices that allow to have *enough* possible paths to fulfill all conditions. The gadget is a graph with  $k + d$  vertices,  $d$  of which are outer vertices and  $k$  are inner vertices. The adjacency matrix of the graph is thus of order  $k + d$ .

**Nonzero contribution. ([Observation 1](#))** We consider a cycle cover consistent with an assignment of the variables. Recall that each boolean variable  $x_i$  is associated to a (blue) cycle in the graph, and that if that a particular cycle is present in the cycle cover then this matches the variable assignment  $x_i = 0$  and if it is not then  $x_i = 1$ . For a gadget representing a clause of degree  $d$  we write  $\mathbf{s}$  the bit-string representing one of the  $2^d$  possible assignments of the variables. The polynomial equation associated to  $\mathbf{s}$  is the permanent of the graph induced by all inner vertices and the outer vertices that are indexed by 1 in  $\mathbf{s}$ , or equivalently the permanent of the adjacency matrix where all rows and columns indexed by 0 in  $\mathbf{s}$  are removed. The polynomial must equate to 1 whenever  $f = 0$ , and  $e^{i\theta}$  for a constant  $\theta \in \mathbb{C}$  otherwise. This naturally induces  $2^d$  equations.

**Zero contribution. ([Observation 2](#))** We consider now a cycle cover inconsistent with an assignment of the variables. When looking only at a traversed gadget, a *partial cycle cover* is a cycle cover with a path entering the gadget in vertex  $x$  and exiting in vertex  $y$  for  $x$  different from  $y$ . We write such a partial cycle cover  $x \rightsquigarrow y$  and the set of all cycle covers of this form  $\mathcal{C}_{x,y}$ . A path  $x \rightarrow y$  (that can traverse any inner vertices and possibly outer vertices) is called a *crossing path* of the partial cycle cover. [Figure 6](#) illustrates two partial cycle covers of the form  $1 \rightsquigarrow 2$ . The term *partial cycle cover* may be misleading; the partial cycle covers are indeed actual cycle covers, but they are partial from the perspective of a single gadget, in the sense that they do not cover the whole gadget. Incidentally, the cycle covers that correspond to a valid assignment of the variables are those that are not *partial* for any gadget of the final graph. This comes from observing that, if a cover partially covers a gadget, then the cycles representing the variable connected to the gadget must also be partially covered (see [Figure 6](#)) and consequently, that cover does not correspond to a valid assignment of the variables. A cycle cover can be seen as a set of oriented pairs of edges representing the arcs (e.g.  $\{\{1, 1\}, \{2, 2\}, \{3, 3\}\}$  for [Figure 1b](#)), hence inclusion is well defined. For a partial cycle cover  $x \rightsquigarrow y$ , we denote by  $\omega(x \rightsquigarrow y)$  the weight of the cycle cover,

*i.e.*, the product of the weights of the edges involved in it. From the above, having captured the notion of inconsistency by partial covers, we can now rephrase [Observation 2](#) as a more formal statement:

*A graph gadget  $A(V_A, E_A)$  is valid if the sum of the weights of all its partial cycle covers is zero.*

Let us denote by  $\mathcal{O}_A \subseteq V_A$  the set of outer vertices of  $A$ . From the perspective of a whole graph  $G(V_G, E_G)$  (in which  $A$  is *included*, *i.e.*,  $V_A \subset V_G$  and  $E_A \subset E_G$ ), the contribution of the partial cycle covers of  $A$  is zero if and only if

$$\sum_{\substack{(x,y) \in \mathcal{O}_A \times \mathcal{O}_A \\ x \neq y}} \left( \sum_{\tilde{c} \in \mathcal{C}_{(x,y)}} \omega(\tilde{c}) \text{Per}(\mathcal{G}_{\tilde{c}}) \right) = 0, \quad (10)$$

where  $G_{\tilde{c}}$  is some graph build upon the graph induced by the edges in the cycle cover  $\tilde{c}$ . Here, the tilde is used to denote partial cycle covers. Designing a valid gadget therefore implies to find the suitable weights of the edges such that the above condition is satisfied. On the one hand, imposing  $\omega(\tilde{c}) = 0$  for all partial cycle cover  $\tilde{c}$  of the gadget is too restrictive, as it would imply that the gadget is not a connected graph, but also that none of the nonzero contribution can be fulfilled. On the other hand, we cannot consider all partial cycle covers at once and simply imposing  $\sum_{\tilde{c}} \omega(\tilde{c}) = 0$ , as this would not imply [Equation \(10\)](#) in the general case.

We denote by  $\mathcal{P}(S)$  the power set of a set  $S$ , and write  $\mathcal{V}_{x,y} = \mathcal{P}(\mathcal{O}_A - \{\{x\}, \{y\}\})$  the set of outer vertices a cycle cover of  $\mathcal{C}_{x,y}$  can traverse. Let  $\mathcal{C}_{x,y}^o \subset \mathcal{C}_{x,y}$  denote the set of partial cycle covers entering in  $x$ , exiting in  $y$  and traversing a set  $o$  of outer vertices, so that

$$\mathcal{C}_{x,y} = \bigcup_{o \in \mathcal{V}_{x,y}} \mathcal{C}_{x,y}^o. \quad (11)$$

The derivation is illustrated via a series of illustrative examples in [Figures 7 to 9](#). The following [Figure 7](#) illustrates the concept of partial cycle covers on a gadget with three outer vertices, for a particular choice of pair  $(x, y)$ .

Let  $c$  be a cycle cover of the full graph and  $\tilde{c}_o \in \mathcal{C}_{x,y}^o$ ,  $\tilde{c}_o \subset c$  be a partial cycle cover of the gadget.  $G_c$  is, in all generality, composed of a component connected to  $x$  and  $y$  which we write  $G_{o,(x,y)}$  and a disconnected component  $G_{\bar{o}}$  (which is connected to all outer vertices not in  $o$ , thus disconnected from the partial cycle cover).  $G_{o,(x,y)}$  indeed contains the edges of  $\tilde{c}_o$  (see [Figure 8](#)).

We now describe how to construct a graph  $G_{o,x \rightarrow y}$  from  $G_{o,(x,y)}$  which will be such that  $\text{Per}(\mathcal{G}_{o,(x,y)}) = \text{Per}(\mathcal{G}_{o,x \rightarrow y}) \omega(\tilde{c}_o)$ .  $G_{o,x \rightarrow y}$  is built from the component connected to  $x$  and  $y$  by removing the edges going from  $x$  and  $y$  to any other vertex

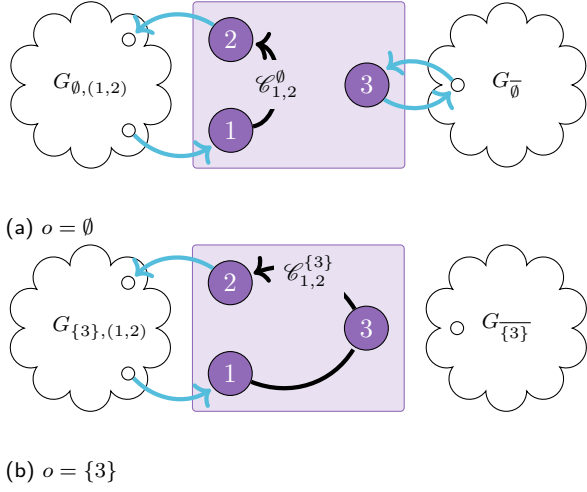


Figure 7: The purple rectangle represents a gadget with three outer vertices, the inner vertices are not shown. For the choice of pair  $(x, y) = (1, 2)$ , Figure 7a (resp. Figure 7b) illustrates sets of partial cycle covers for the choice of outer vertices  $o = \emptyset$  (resp.  $o = \{3\}$ ).

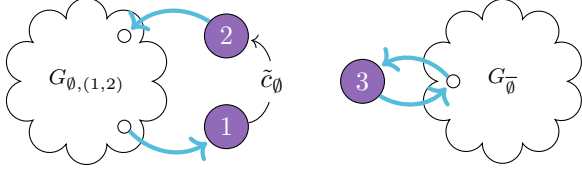


Figure 8: Following the example of Figure 7, we set  $o = \emptyset$ , which in turn sets  $G_{\emptyset, (1,2)}$  and  $G_{\overline{\emptyset}}$ . Then, we choose a particular partial cycle cover  $\tilde{c}_{\emptyset} \in \mathcal{C}_{1,2}^{\emptyset}$ .

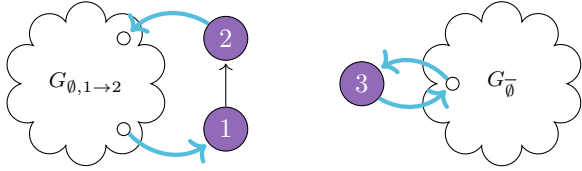


Figure 9: Continuing with the example initiated in Figure 8, we build  $G_{\emptyset, 1 \rightarrow 2}$  from  $G_{\emptyset, (1,2)}$  by removing the edges arriving in vertices 1 and 2 to any vertex of the gadget, and adding the edge  $1 \rightarrow 2$  of weight 1.

in  $A$  and adding the edge  $x \rightarrow y$  of weight one (see Figure 9).

Overall, the weight of the cycle cover  $c$  is  $\text{Per}(\mathcal{G}_{o, x \rightarrow y}) \text{Per}(\mathcal{G}_{\overline{o}}) \omega(\tilde{c}_o)$ . We can observe that  $\text{Per}(\mathcal{G}_{o, x \rightarrow y}) \text{Per}(\mathcal{G}_{\overline{o}})$  remains unchanged for any choice of  $\tilde{c}_o$  for fixed  $o$ . In that regard, Equation (10) rewrites

$$\sum_{\substack{(x,y) \in \mathcal{O}_A^2 \\ x \neq y}} \sum_{\substack{o \in \mathcal{V}_{x,y} \\ o \neq \emptyset}} \left( \text{Per}(\mathcal{G}_{o, x \rightarrow y}) \text{Per}(\mathcal{G}_{\overline{o}}) \right) \times \sum_{\tilde{c}_o \in \mathcal{C}_{x,y}^o} \omega(\tilde{c}_o) = 0. \quad (12)$$

While designing a gadget with fixed number of inner vertices, the only control one has is on the weights

$\omega(\tilde{c}_o)$ , as all the other terms of Equation (12) depend on a specific instance. But still, one must ensure that Equation (12) holds. Hence, in order to design a clause gadget whose supposedly zero contributions are effectively zero, one must ensure that, for all  $(x, y) \in \mathcal{O}_A \times \mathcal{O}_A$  with  $x \neq y$  and for all  $o \in \mathcal{P}(\mathcal{O}_A - \{\{x\}, \{y\}\})$ , the following holds

$$\sum_{\tilde{c}_o \in \mathcal{C}_{x,y}^o} \omega(\tilde{c}_o) = 0. \quad (13)$$

Applying Equation (13) to the example of Figure 7 for the fixed pair  $(1, 2)$  yields:

$$\sum_{\tilde{c}_{\emptyset} \in \mathcal{C}_{1,2}^{\emptyset}} \omega(\tilde{c}_{\emptyset}) = \sum_{\tilde{c}'_{\{3\}} \in \mathcal{C}_{1,2}^{\{3\}}} \omega(\tilde{c}'_{\{3\}}) = 0. \quad (14)$$

Consequently, a gadget  $A$  might require several inner vertices to have enough degrees of freedom (the supplementary nodes and the weights on their connected edges) to satisfy Equation (13). Note that it does not show that grouping the partial cycle cover with respect to the set of outer vertices they traverse is the most efficient way to design a gadget, in the sense that there might be a way to group them in bigger groups, therefore lowering the number of inner vertices required. However, Equation (12) seems to indicate that this choice is optimal as we only have a local control on each contribution (the  $\omega(\tilde{c})$ 's).

The construction of the system of equations for the zero contributions is slightly more involved than the nonzero case. Given two outer vertices  $x$  and  $y$  in  $\mathcal{O}_A$ , we want that all the partial cycle covers of  $\mathcal{C}_{x,y}$  have zero contribution. In order to write the constraints on the contributions of all partial covers  $\mathcal{C}_{x,y}$  – comprising the paths  $x \rightarrow y$  – as permanent equations we use the following trick. Given  $x$  and  $y$ , we set to 0 all the entries of the  $y$ -th row of the adjacency matrix, apart from the  $x$ -th entry that we set to 1. This way, all edges exiting  $y$  are removed and an artificial edge  $y \rightarrow x$  is created, so that all crossing paths  $x \rightarrow y$  are transformed into cycles. As a result, the permanent of the remaining graph is exactly the sum of all the contributions of the partial covers of  $\mathcal{C}_{x,y}$ . Recall that we grouped the covers in  $\mathcal{C}_{x,y}$  according to the set of outer vertices they traverse (see Equation (11)), hence this procedure is applied *separately* to such set. From a pair  $(x, y)$  and a set of outer vertices, the procedure generates a single polynomial. We repeat this procedure for all pairs of outer vertices, and we obtain a system of  $2^{d-2}d(d-1)$  equations. The overall procedure to generate the system of equations is summarized in Algorithm 1, and the resulting system of polynomial equations is characterized in the following Proposition 1. Observe that the algorithm does no computation, *i.e.*, no permanent is computed, but the variables are symbolically manipulated to write down polynomials. Theorem 1 asserts that whether a desired design is possible can be decided by com-

---

**Algorithm 1:** Procedure for the generation of the clause gadget constraints

---

**inputs :**

- $d$  the degree of the clause,
- $k$  the number of inner degrees of freedom,
- $m$  a clause of degree  $d$ .

**output:** The family of polynomial equations associated to the input parameters.

**begin**

Let  $F$  be the list of polynomials.  
 Let  $A(V_A, E_A)$  be the symbolic gadget with adjacency matrix  $\mathcal{A} := (x_{ij})_{1 \leq i, j \leq k+d}$ .  
 Let  $\mathcal{O}$  (resp.  $\mathcal{I}$ ) be the set of outer (resp. inner) vertices indexes of  $A(V_A, E_A)$  (i.e.,  $V_A = \mathcal{O} \cup \mathcal{I}$ ).

**for all**  $s \in \{0, 1\}^d$  **do**

$\mathcal{O}_s \leftarrow \{i \mid i \in \mathcal{O}, s_i = 1\}$   
 $A'(V'_A, E'_A) \leftarrow A'(\mathcal{O}_s \cup \mathcal{I}, E_A)$ ;  $\triangleright E_{A'}$   
 is the set of edges of  $A$  induced by the vertices in  $\mathcal{O}_s \cup \mathcal{I}$   
 $F \leftarrow F \cup \text{Per}(\mathcal{A}') - e^{im}$

**end**

**for all**  $(x, y) \in \mathcal{O} \times \mathcal{O}$  s.t.  $x \neq y$  **do**

**for**  $v \in \mathcal{V}_{x,y}$  **do**  
 $A''(V''_A, E''_A) \leftarrow A''(\{x, y\} \cup v \cup \mathcal{I}, E_{A'})$   
 Set the row representing  $y$  to zero, apart from the  $x$ -th entry that is set to 1 in  $A''$ .  
 $F \leftarrow F \cup \text{Per}(\mathcal{A}'')$

**end**

**end**

**return**  $F$

**end**

---

putting the reduced Gröbner basis of the system of polynomials.

**Theorem 1** (Gadget existence). *There exists a gadget encoding the clause*

$$m = \theta \prod_{\substack{i \in S \\ S \subseteq [n] \\ |S|=d}} x_i \quad (15)$$

with  $d+k$  vertices if and only if the system of polynomial equations created by Algorithm 1 on parameters  $d, k$  and  $m$  has a reduced Gröbner basis different from  $\{1\}$ .

*Proof.* The proof follows from Hilbert's Nullstellensatz [20, see Chapter 4] and the correctness of Algorithm 1.

*Proof of correctness of Algorithm 1.* The first for all loop writes all the constraints related to Observation 1. The second for all loop tweaks the graph to

match Equation (13) and write the constraints related to Observation 2.

*Proof of gadget existence.* Let  $F$  be the system of polynomial equations generated by Algorithm 1 on parameters  $d, k$  and  $m$ . If the reduced Gröbner basis of  $\langle F \rangle$  is not  $\{1\}$ , then  $F$  has (at least) a solution.  $\square$

Besides its existence, the construction of such a gadget is ensured by the elimination theory [20, see Chapter 3], provided the reduced Gröbner basis is computed with respect to an elimination order. A point  $\mathbf{x} = (x_1, \dots, x_{(k+d)^2})$  such that  $F(\mathbf{x}) = 0$  corresponds to the entries of the adjacency matrix of the gadget. Incidentally, we have the following Corollary 1.

**Corollary 1** (Smallest graph gadget). *The optimal value of  $k$  to design a gadget is the smallest integer such that the reduced Gröbner basis of the system of polynomial equations generated by Algorithm 1 on parameters  $d, k$  and  $m$  is not  $\{1\}$ .*

**Proposition 1** (Characterisation of the system of equations). *Let  $A$  be the adjacency matrix of a gadget representing a clause of degree  $d$  with  $k$  inner degrees of freedom. Then, the Algorithm 1 generates a system of  $2^d (d(d-1)2^{-2} + 1)$  multilinear polynomial equations in  $(k+d)^2$  variables. It runs in time  $\Theta(2^d)$ .*

*Proof.* Each entry of the  $(k+d) \times (k+d)$  adjacency matrix of the gadget is a variable hence the number of variables in the polynomial system is  $(k+d)^2$ . The first for all loop of Algorithm 1 generates  $2^d$  equations, and the second generates  $2^{d-2}d(d-1)$ .  $\square$

A drawback of Algorithm 1 is that the set of polynomial  $F$  contains a lot of redundancy. Therefore, in practice before computing the reduced Gröbner basis of a system of polynomial equations, we advise using Laplace's expansion formula along a row, which reads for the  $i$ -th

$$\text{Per}(A) = \sum_{j=1}^n a_{i,j} \text{Per}(A_{\bar{i},\bar{j}}), \quad (16)$$

where  $A_{\bar{i},\bar{j}}$  is the submatrix of  $A$  obtained by removing the  $i$ -th row and the  $j$ -th column. This relies on the fact that Algorithm 1 sets the value of many submatrix permanents  $\text{Per}(A_{\bar{i},\bar{j}})$ , which can then be substituted in the rest of the system. If a numerical solution is sought, one can use homotopy continuation [23], as many computer algebra system do not implement solution finding from the reduced Gröbner basis over the complex numbers when the variety is not zero-dimensional [24, 25]. Finding a solution, that is, a clause gadget, takes exponential time [22], but is an operation that only has to be done once for each degree. Also, it is to be noted that both polynomial time encodings of [4, 13] do not take into account the computational complexity of the task of finding a gadget.

### 3.2 Computation of some graph gadgets and application to quantum circuits amplitude computation

In this section, we give an illustrative example by deriving the graph gadgets for linear, quadratic and cubic clauses, and show how this can be applied to quantum circuit probability amplitudes computation.

**Gadget computation.** We denote by  $A_k(\theta)$  the adjacency matrix of the gadget encoding a clause of degree  $k$  with coefficient  $\theta$ . Its and  $k$  first rows/columns index the outer vertices of the gadget, while the remaining ones indicate the inner vertices. The following gadgets are derived by solving the system of equations returned by [Algorithm 1](#) on the appropriate parameters. The computations were performed using the Julia programming language [25, 26]. The degree-one monomials with coefficient  $\theta$  are encoded into the following gadget represented by a  $1 \times 1$  matrix:

$$A_1(\theta) := [e^{i\theta}].$$

The quadratic clauses with coefficient  $\theta$  are encoded into a gadget with one inner vertex:

$$A_2(\theta) := \begin{bmatrix} \frac{1}{2}(1 + e^{i\theta}) & \frac{1}{2}(e^{i\theta} - 1) & \frac{1}{2}(1 - e^{i\theta}) \\ -1 & 0 & 1 \\ 1 & 1 & 1 \end{bmatrix}.$$

Finally, the cubic clauses with coefficient are encoded into the following gadget comprising two inner vertices. Let  $\eta(\theta) := \frac{1}{6}\sqrt{3(1+i)(1-e^{i\theta})}$ ,

$$A_3(\theta) := \begin{bmatrix} \frac{e^{i\theta} - (1+12i)}{-12i} & -\eta(\theta) & -\eta(\theta) & \frac{\eta(\theta)}{\sqrt{2}}e^{i\frac{\pi}{4}} & \frac{-\eta(\theta)}{\sqrt{2}} \\ -\eta(\theta) & i & -1+i & 1 & e^{i\frac{3\pi}{4}} \\ -\eta(\theta) & -1+i & i & 1 & e^{i\frac{3\pi}{4}} \\ \frac{\eta(\theta)}{\sqrt{2}}e^{i\frac{\pi}{4}} & 1 & 1 & 1 & 0 \\ -\sqrt{\frac{(1-e^{i\theta})}{24(1+i)}} & e^{i\frac{3\pi}{4}} & e^{i\frac{3\pi}{4}} & 0 & 1 \end{bmatrix}.$$

Foremost, for each gadget the number of inner vertices is minimal according to [Corollary 1](#).

**Quantum circuits.** These gadgets can be used to encode probability amplitudes of a broad family of quantum circuits, we exemplify with an IQP circuit. A simple gate-set, which comes with hardness results regarding classical simulation is that of Instantaneous Quantum Polynomial-time (IQP) circuits [27, 28, 29]. IQP circuits are circuits  $\mathcal{C} = H^{\otimes q} \mathcal{D} H^{\otimes q}$ , with  $\mathcal{D}$  diagonal in the  $Z$ -basis. They were introduced as a subset of quantum circuits that is rich enough to enable sampling from distributions that is hard to describe classically.

We shall call a *balanced* gate any gate  $\mathcal{U}(\theta)$  whose amplitudes are of the form

$$\langle \mathbf{y} | \mathcal{U}(\theta) | \mathbf{x} \rangle = \begin{cases} 0 & \text{or} \\ \frac{e^{i\theta f(\mathbf{x}, \mathbf{y})}}{\sqrt{M}} \end{cases}, \quad (17)$$

where  $M$  is the number of states  $|\mathbf{y}\rangle$  such that  $\langle \mathbf{y} | \mathcal{U} | \mathbf{x} \rangle$  is nonzero and  $f \in \mathbb{F}_2[\mathbf{x}, \mathbf{y}]$  is a polynomial. Here, *balanced* indicates that all amplitudes have the same magnitude. Examples of gates satisfying [Equation \(17\)](#) are the (arbitrary controlled) phase gates ( $M = 1$ ), defined as

$$P_k(\theta) : |x_1, \dots, x_k\rangle \mapsto e^{i\theta \prod_{j=1}^k x_j} |x_1, \dots, x_k\rangle, \quad (18)$$

for all  $k \geq 1$  and  $x_j \in \{0, 1\}$  for all  $1 \leq j \leq k$ , or the Hadamard gates ( $\theta = \pi$ ,  $M = 2$ ). Suitable gate-sets for  $\mathcal{D}$  could be  $\{P_0(\frac{\pi}{8}), P_1(\frac{\pi}{4})\}$  or  $\{P_k(\pi) | k = 0, 1, 2\}$  [29]. The polynomial  $f$  is a function of the computational basis bit-strings, in which each variable is either raised to the zeroth or the first power, *i.e.*, a clause of degree  $d$  contains  $d$  distinct variables – so that the resulting polynomial is a multilinear polynomial of degree  $d$ . Probability amplitudes of quantum circuits built upon balanced gates can be straightforwardly encoded onto a graph. Using encoding of quantum circuit amplitudes onto polynomials [11, 30] and the gadgets we derived, each  $P_k(\theta)$  gate is to be encoded into a gadget  $A_k(\theta)$ . The resulting graph is a graph  $G_{\mathcal{C}}(V, E)$  such that

$$\langle \mathbf{a} | \mathcal{C} | \mathbf{b} \rangle = \frac{1}{\sqrt{2^h}} \sum_{\mathbf{x}} e^{if(\mathbf{x})} = \frac{1}{\sqrt{2^h}} \text{Per}(G_{\mathcal{C}}). \quad (19)$$

Remark that  $A_2(\pi)$  is the gadget encoding the quadratic clauses of [13], which is consistent with the observation that both Hadamard (regardless its rescaling factor) and CZ amplitudes are of the form  $(-1)^{xy}$  for the suitable choice of variables  $x$  and  $y$ . The encoding of [13] therefore comes as a special case of our method.

With these three gadgets in hand, the graph encoding of  $q$ -qubit IQP circuits is characterized by the following [Proposition 2](#). Throughout rest, let  $\#(\mathcal{U})$  denote the number of occurrences of the gate  $\mathcal{U}$  in the circuit  $\mathcal{C}$ , *e.g.*,  $\#(H) = 2q$ .

**Proposition 2** (Size of the resulting graph). *Let  $\mathcal{C}$  be a  $q$ -qubit IQP circuit of depth  $d$  and  $G_{\mathcal{C}}(V, E)$  be the graph such that  $\langle 0^{\otimes q} | \mathcal{C} | 0^{\otimes q} \rangle = \frac{1}{2^q} \text{Per}(G_{\mathcal{C}})$ . Then,  $G_{\mathcal{C}}$  is a graph with*

$$M = q + \#(P_0(\theta)) + 3\#(P_1(\theta)) + 5\#(P_2(\theta)) \quad (20)$$

vertices.

*Proof.* The proof simply follows from counting the number of nodes of each gadget.  $\square$

**Example.** For the example, we consider the 3-qubit circuit depicted in [Figure 10](#) which we call  $\mathcal{C}$ . Following the method for creating the variables on the circuit wires, we have 9 variables. Write  $\mathbf{x} = (x_0, \dots, x_8)$ , the polynomial associated to  $\mathcal{C}$  is

$$f(\mathbf{x}) = \sum_{i=0}^5 \pi x_i x_{i+3} + \theta_3 x_3 x_4 x_5 + \theta_2 x_3 x_4 + \theta_1 x_5. \quad (21)$$



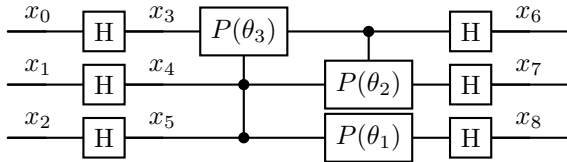


Figure 10: Example 3-qubit circuit with its associated variables  $x_0, \dots, x_8$ .

and the amplitude as function of the variables reads

$$\langle x_6, x_7, x_8 | \mathcal{C} | x_0, x_1, x_2 \rangle = \frac{1}{2^3} \sum_{\mathbf{x}} e^{if(\mathbf{x})}. \quad (22)$$

For the sake of the example, let's compute the amplitude  $\langle 0^{\otimes 3} | \mathcal{C} | 0^{\otimes 3} \rangle$  via the graph encoding, *i.e.*, set all the variables but  $x_3, x_4, x_5$  to zero. Also, set arbitrarily  $\theta_1 := \frac{\pi}{2}$ ,  $\theta_2 := \frac{\pi}{4}$  and  $\theta_3 := \frac{\pi}{8}$ . Then, construct the graph from the gadgets  $A_i(\theta_i)$ ,  $i = 0, 1, 2$ ; it is shown in Figure 11. Note that since the variables encoding the amplitude are set to zero, a slightly more economical encoding is possible for all the clauses involving these variables as there is no polynomial to evaluate (see Equation (17)): it is the constant polynomial 0. Finally, we compute the permanent of  $\mathcal{G}_{\mathcal{C}}$  to get the amplitude. Numerical computation yields

$$\langle 0^{\otimes 3} | \mathcal{C} | 0^{\otimes 3} \rangle = \frac{1}{8} \text{Per}(\mathcal{G}_{\mathcal{C}}) \approx (0.348 + 0.511i). \quad (23)$$

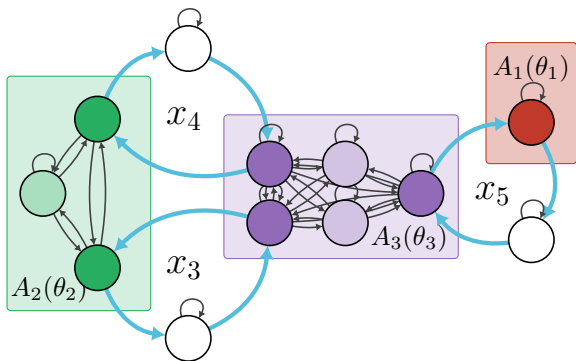


Figure 11: Graph encoding of the circuit of Figure 10. The gadget labelled  $A_k(\theta_k)$  results from the encoding of the  $P_k(\theta_k)$  gate. The blue edges have weight 1, and the adjacency matrices of the graph gadgets  $A_k(\theta_k)$  were given earlier in Section 3.2. We encode the zeros in the input and output using a similar economical encoding as proposed in [13, Note Ref. 10], *i.e.*, via self-loops of weight 1 (the white nodes).

## 4 Applications

**Classical simulation.** The encoding constructs sparse graphs, even in the general case, and even with gadget we do not know yet the design of, as it constructs a matrix with blocks of constant size

in its diagonal linked together with a constant number of edges. As such, we can use the algorithm of [31], which allows to compute the permanent of sparse  $n \times n$  matrices with  $Cn$  nonzero entries in time  $(2 - \varepsilon)^n$  for some strictly positive constant  $\varepsilon$  and space  $\mathcal{O}(n)$ . This is indeed better than Ryser's  $\mathcal{O}(2^n)$  formula [32] for exact computation, or Gurvits' approximate algorithm [15], which, given  $A$  of order  $n$ , computes an estimate of  $\text{Per}(A)$  to within additive error  $\pm \varepsilon \|A\|_2^n$  in time  $\mathcal{O}(n^2 \varepsilon^{-2})$ . Because the cycles linking the gadgets and representing the variables must have weight 1, we have  $\|A\|_2 \geq 1$  [33]. Incidentally, the connected components of the graph one obtains from the encoding are correlated with the set of qubits interacting together. Recall that for the matrix  $A = \text{diag}(A_2, \dots, A_k)$  with  $A_i$  a square matrix for all  $1 \leq i \leq k$ ,

$$\text{Per}(A) = \prod_{i=1}^k \text{Per}(A_i). \quad (24)$$

This can be combined with [31] to further speed up the computation. However, in practice, for random  $q$ -qubit circuits of depth  $d$  build upon 2-qubit gates, there are  $\mathcal{O}(1)$  blocks as soon as  $d = \mathcal{O}(\log q)$ .

**Quantum simulation.** A natural question that arises is how the method developed above compares against the standard gate-based implementation in linear optics following the KLM scheme [34]. In Appendix B, we benchmark the graph encoding against the KLM scheme and our encoding is found to be less demanding, both in terms of samples and single photons per shot. We formally show that this holds and the results culminate in Theorem 1 in Appendix B.1.2 and Theorem 2 in Appendix B.2. The empirical bound of 44 qubits, where we expect improvement with almost unit probability, is outside the scope of current simulators capabilities [35]. We believe similar bounds could be obtained for other sets of gates, as the probabilistic nature of linear optical multi-qubit gates plays in our favour.

## 5 Conclusion

We have provided a method to compute sums of exponentiated polynomials as matrix permanents. This technique finds its application in the encoding of quantum circuits amplitudes. This yields a general extension of the encoding of quantum circuit output amplitudes as graph permanents of [13], unifying this graph-encoding with polynomial expression of quantum circuit amplitudes as in [30]. To achieve this, we have shown that a clause gadget can be found by solving a system of multilinear polynomial equations through Gröbner basis theory. While hard in general, this computation has only to be done once per degree, providing a parameterized gadget for the clauses of

that degree. Additionally, we remark that the nice structure of the graph opens the door to permanent-based classical methods for the simulation of quantum circuits [31, 32, 36].

## Acknowledgements

The authors warmly thank Ulysse Chabaud and Shane Mansfield for the valuable feedback on the manuscript and Elham Kashefi for the fruitful discussions. This work has been co-funded by the European Commission as part of the EIC accelerator program under the grant agreement 190188855 for SEPOQC project, by the Horizon-CL4 program under the grant agreement 101135288 for EPIQUE project.

## References

- [1] Nicolas Maring, Andreas Fyrillas, Mathias Pont, Edouard Ivanov, Petr Stepanov, Nico Margaria, William Hease, Anton Pishchagin, Aristide Lemaître, Isabelle Sagnes, Thi Huong Au, Sébastien Boissier, Eric Bertasi, Aurélien Baert, Mario Valdivia, Marie Billard, Ozan Acar, Alexandre Brioussel, Rawad Mezher, Stephen C. Wein, Alexia Salavrakos, Patrick Sinnott, Dario A. Fioretto, Pierre-Emmanuel Emeriau, Nadia Belabas, Shane Mansfield, Pascale Senellart, Jean Senellart, and Niccolo Somaschi. “A versatile single-photon-based quantum computing platform”. *Nature Photonics* (2024).
- [2] Sara Bartolucci, Patrick Birchall, Hector Bombín, Hugo Cable, Chris Dawson, Mercedes Gimeno-Segovia, Eric Johnston, Konrad Kieling, Naomi Nickerson, Mihir Pant, Fernando Pastawski, Terry Rudolph, and Chris Sparrow. “Fusion-based quantum computation”. *Nature Communications* **14**, 912 (2023).
- [3] Scott Aaronson and Alex Arkhipov. “The computational complexity of linear optics”. In Proceedings of the forty-third annual ACM symposium on Theory of computing. Pages 333–342. San Jose California USA (2011). ACM.
- [4] L.G. Valiant. “The complexity of computing the permanent”. *Theoretical Computer Science* **8**, 189–201 (1979).
- [5] Kaifeng Bu and Dax Enshan Koh. “Classical Simulation of Quantum Circuits by Half Gauss Sums”. *Communications in Mathematical Physics* **390**, 471–500 (2022).
- [6] Jin-Yi Cai, Xi Chen, Richard Lipton, and Pinyan Lu. “On tractable exponential sums”. In *Frontiers in Algorithmics*. Pages 148–159. Springer (2010).
- [7] Enrico Bombieri. “On Exponential Sums in Finite Fields”. *American Journal of Mathematics* **88**, 71–105 (1966).
- [8] N. M. Korobov. “Weyl’s sums”. Pages 68–138. Springer Netherlands. (1992).
- [9] Larry Stockmeyer. “The complexity of approximate counting”. In Proceedings of the fifteenth annual ACM symposium on Theory of computing - STOC ’83. Pages 118–126. ACM Press (1983).
- [10] R. P. Feynman, A. R. Hibbs, and George H. Weiss. “*Quantum Mechanics and Path Integrals*”. *Physics Today* **19**, 89–89 (1966).
- [11] Christopher M. Dawson, Andrew P. Hines, Duncan Mortimer, Henry L. Haselgrove, Michael A. Nielsen, and Tobias J. Osborne. “Quantum computing and polynomial equations over the finite field  $\mathbb{Z}_2$ ”. *Quantum Info. Comput.* **5**, 102–112 (2005).
- [12] Andrzej Ehrenfeucht and Marek Karpinski. “The computational complexity of (xor, and)-counting problems”. *International Computer Science Inst.* (1990).
- [13] Terry Rudolph. “Simple encoding of a quantum circuit amplitude as a matrix permanent”. *Physical Review A* **80**, 054302 (2009).
- [14] Leonid Gurvits. “On the complexity of mixed discriminants and related problems”. In Joanna Jedrzejowicz and Andrzej Szepietowski, editors, *Mathematical Foundations of Computer Science 2005*. Pages 447–458. Springer Berlin Heidelberg (2005).
- [15] Scott Aaronson and Travis Hance. “Generalizing and Derandomizing Gurvits’s Approximation Algorithm for the Permanent” (2012).
- [16] Markus Bläser, Holger Dell, and Mahmoud Fouz. “Complexity and approximability of the cover polynomial”. *computational complexity* **21**, 359–419 (2012).
- [17] Rawad Mezher, Ana Filipa Carvalho, and Shane Mansfield. “Solving graph problems with single photons and linear optics”. *Phys. Rev. A* **108**, 032405 (2023).
- [18] Marvin Marcus and Henryk Minc. “Permanents”. *The American Mathematical Monthly* **72**, 577 (1965).
- [19] Scott Aaronson. “A Linear-Optical Proof that the Permanent is #P-Hard”. *Proceedings of the Royal Society A: Mathematical, Physical and Engineering Sciences* **467**, 3393–3405 (2011).
- [20] David Cox, John Little, and Donal OShea. “Ideals, varieties, and algorithms: an introduction to computational algebraic geometry and commutative algebra”. Springer Science & Business Media. (2013).
- [21] Jean Charles Faugère. “A new efficient algorithm for computing gröbner bases without reduction to zero (f5)”. In Proceedings of the 2002 international symposium on Symbolic and algebraic computation. Pages 75–83. ISSAC ’02. Association for Computing Machinery (2002).

- [22] Magali Bardet, Jean-Charles Faugère, and Bruno Salvy. “On the complexity of the F5 Gröbner basis algorithm”. *Journal of Symbolic Computation* **70**, 49–70 (2015).
- [23] Tianran Chen and Tien-Yien Li. “Homotopy continuation method for solving systems of nonlinear and polynomial equations”. *Communications in Information and Systems* **15**, 119–307 (2015).
- [24] Jérémy Berthomieu, Christian Eder, and Mohab Safey El Din. “msolve: A Library for Solving Polynomial Systems”. In 2021 International Symposium on Symbolic and Algebraic Computation. Pages 51–58. 46th International Symposium on Symbolic and Algebraic Computation Saint Petersburg, Russia (2021). ACM.
- [25] Alexander Demin and Shashi Gowda. “Groebner.jl: A package for gröbner bases computations in julia”. *arXiv preprint arXiv:2304.06935* (2023).
- [26] Jeff Bezanson, Alan Edelman, Stefan Karpinski, and Viral B. Shah. “Julia: A Fresh Approach to Numerical Computing”. *SIAM Review* **59**, 65–98 (2017).
- [27] Dan Shepherd and Michael J. Bremner. “Temporally unstructured quantum computation”. *Proceedings of the Royal Society A: Mathematical, Physical and Engineering Sciences* **465**, 1413–1439 (2009).
- [28] Michael J. Bremner, Richard Jozsa, and Dan J. Shepherd. “Classical simulation of commuting quantum computations implies collapse of the polynomial hierarchy”. *Proceedings of the Royal Society A: Mathematical, Physical and Engineering Sciences* **467**, 459–472 (2011).
- [29] Michael J. Bremner, Ashley Montanaro, and Dan J. Shepherd. “Average-case complexity versus approximate simulation of commuting quantum computations”. *Physical Review Letters* **117** (2016).
- [30] Ashley Montanaro. “Quantum circuits and low-degree polynomials over  $\mathbb{F}_2$ ”. *Journal of Physics A: Mathematical and Theoretical* **50**, 084002 (2017).
- [31] Rocco A. Servedio and Andrew Wan. “Computing sparse permanents faster”. *Information Processing Letters* **96**, 89–92 (2005).
- [32] H.J. Ryser. “Combinatorial mathematics”. *Carus mathematical monographs*. Mathematical Association of America. (1973).
- [33] Suk-Geun Hwang. “Cauchy’s Interlace Theorem for Eigenvalues of Hermitian Matrices”. *The American Mathematical Monthly* **111**, 157 (2004).
- [34] E Knill, R Laflamme, and G Milburn. “A scheme for efficient quantum computation with linear optics”. *Nature* **409**, 46–52 (2001).
- [35] Nicolas Heurtel, Andreas Fyrrillas, Grégoire De Gliniasty, Raphaël Le Bihan, Sébastien Malherbe, Marceau Pailhas, Eric Bertasi, Boris Bourdoncle, Pierre-Emmanuel Emeriau, Rawad Mezher, Luka Music, Nadia Belabas, Benoît Valiron, Pascale Senellart, Shane Mansfield, and Jean Senellart. “Perceval: A Software Platform for Discrete Variable Photonic Quantum Computing”. *Quantum* **7**, 931 (2023).
- [36] Mark Jerrum, Alistair Sinclair, and Eric Vigoda. “A polynomial-time approximation algorithm for the permanent of a matrix with nonnegative entries”. *J. ACM* **51**, 671–697 (2004).
- [37] Roger A. Horn and Charles R. Johnson. “Matrix analysis”. *Cambridge University Press*. Cambridge (2012). 2nd ed edition.
- [38] Baodong Zheng and Liancheng Wang. “Spectral radius and infinity norm of matrices”. *Journal of Mathematical Analysis and Applications* **346**, 243–250 (2008).
- [39] David Carlson. “Minimax and interlacing theorems for matrices”. *Linear Algebra and its Applications* **54**, 153–172 (1983).
- [40] E. Knill. “Quantum gates using linear optics and postselection”. *Physical Review A* **66**, 052306 (2002).
- [41] Wassily Hoeffding. “Probability Inequalities for Sums of Bounded Random Variables”. *Journal of the American Statistical Association* **58**, 13–30 (1963).
- [42] Holger F. Hofmann and Shigeki Takeuchi. “Quantum phase gate for photonic qubits using only beam splitters and postselection”. *Physical Review A* **66**, 024308 (2002).
- [43] Michael A. Nielsen and Isaac L. Chuang. “Quantum Computation and Quantum Information: 10th Anniversary Edition”. *Cambridge University Press*. (2010).
- [44] Vivek V. Shende and Igor L. Markov. “On the CNOT-cost of TOFFOLI gates” (2008). *arXiv:0803.2316 [quant-ph]*.
- [45] T. C. Ralph, K. J. Resch, and A. Gilchrist. “Efficient Toffoli Gates Using Qudits”. *Physical Review A* **75**, 022313 (2007).
- [46] Qing Lin and Jian Li. “Quantum control gates with weak cross-Kerr nonlinearity”. *Physical Review A* **79**, 022301 (2009).
- [47] Lee-Ad Gottlieb, Aryeh Kontorovich, and Elchanan Mossel. “VC bounds on the cardinality of nearly orthogonal function classes”. *Discrete Mathematics* **312**, 1766–1775 (2012).

## A Linear algebra

This paragraph outlines the linear-algebra tools and notation used throughout this work. We use bold fonts for a shorthand notation of vectors:  $\mathbf{x} = (x_1, \dots, x_n)$ . The singular value decomposition of a matrix  $A \in \mathbb{C}^{m \times n}$  is

a factorization of  $A$  into the product of three matrices  $U\Sigma V^*$ , where the columns of  $U$  and  $V$  are orthonormal and  $\Sigma = \text{diag}(\sigma_1, \dots, \sigma_n)$  is a diagonal matrix with positive real entries –  $A$ 's *singular values*. For a matrix  $A \in \mathbb{C}^{m \times n}$ ,  $\|A\|_p$  denotes the matrix norm induced by the vector  $p$ -norm, for  $p \in [1, \infty]$ , defined as

$$\|A\|_p = \sup_{x \neq 0} \frac{\|Ax\|_p}{\|x\|_p}. \quad (25)$$

Special cases of  $p = 1, 2, \infty$  are

$$\|A\|_1 = \max_{1 \leq j \leq n} \sum_{i=1}^m |a_{ij}|, \quad (26a)$$

$$\|A\|_2 = \sigma_{\max}(A), \quad (26b)$$

$$\|A\|_\infty = \max_{1 \leq i \leq m} \sum_{j=1}^n |a_{ij}|, \quad (26c)$$

where  $\sigma_{\max}(A)$  denotes the largest singular value of  $A$ . The function  $\|\cdot\|_p$  is sub-additive [37], *i.e.*,  $\|A+B\|_p \leq \|A\|_p + \|B\|_p$  for all  $p \in [1, \infty]$ . Let  $\lambda_1, \dots, \lambda_n$  be the eigenvalues of  $A$ , the *spectral radius* of  $A$  is defined as

$$\rho(A) = \max\{|\lambda_1|, \dots, |\lambda_n|\}. \quad (27)$$

It follows that  $\|A\|_2 = \rho(A^*A)$  where  $A^*$  denotes the conjugate transpose of  $A$  and  $\rho(A) \leq \|A\|_\infty$  for any real-valued matrix  $A$  [38]. The notation  $\text{diag}$  is extended to matrices, *i.e.*, the block diagonal matrix  $A$  with blocks  $A^{(1)}, \dots, A^{(k)}$  is written

$$A = \text{diag}\left(\{A^{(j)}\}_{j=1}^k\right), \quad (28)$$

with  $A^{(j)}$  an  $n_j \times n_j$  matrix and  $\sum_{j=1}^k n_j = n$ .

Finally, we will use Cauchy's interlacing theorem for the eigenvalues of Hermitian matrices [39], which states that, assuming  $A \in \mathbb{C}^{n \times n}$  is Hermitian and  $B \in \mathbb{C}^{m \times m}$  with  $m < n$  is a principal submatrix of  $A$ , suppose  $A$  has eigenvalues  $\alpha_1 \geq \dots \geq \alpha_n$  and  $B$  has eigenvalues  $\beta_1 \geq \dots \geq \beta_m$ , then, for all  $k = 1, \dots, m$ , the eigenvalues of  $B$  interlace those of  $A$ , *i.e.*,

$$\alpha_k \geq \beta_k \geq \alpha_{k+n-m}. \quad (29)$$

## B Benchmark of the scheme and comparison with non-adaptive KLM

Linear optical quantum computation involves  $n$  identical photons evolving in  $m$  modes. Each computational basis state is of the form  $|\mathbf{s}\rangle = (s_1, \dots, s_m)$  with  $\sum_{i=1}^m s_i = n$ ,  $s_i \geq 0$  is the number of photons in mode  $i$ . The evolution of state  $\mathbf{s}$  undergoing the transformation induced by a linear optical circuit is described by a unitary operator  $\mathcal{U}$  acting on the state  $\mathbf{s}$ , we have

$$\langle \mathbf{t} | \mathcal{U} | \mathbf{s} \rangle = \frac{\text{Per}(\mathcal{U}_{\mathbf{s}, \mathbf{t}})}{\sqrt{\mathbf{s}! \mathbf{t}!}}. \quad (30)$$

On the one hand, it was shown in [17] that it is possible to encode the adjacency matrix of a graph  $G(V, E)$  onto a unitary matrix  $\mathcal{U}$  such that

$$\langle \mathbf{1}_n | \mathcal{U} | \mathbf{1}_n \rangle \propto \text{Per}(\mathcal{G}), \quad (31)$$

where  $|\mathbf{1}_n\rangle = |1^{\otimes n} 0^{\otimes m-n}\rangle$ . In particular, let  $\mathcal{C}$  be a quantum circuit and  $G_{\mathcal{C}}(V, E)$  be the graph encoding the amplitude  $\langle \mathbf{b} | \mathcal{C} | \mathbf{a} \rangle$  for  $\mathbf{a}, \mathbf{b} \in \{0, 1\}^n$ , then it is possible to encode the adjacency matrix  $\mathcal{G}_{\mathcal{C}}$  into a linear optical circuit  $\mathcal{V}$  such that

$$\langle \mathbf{1}_n | \mathcal{V} | \mathbf{1}_n \rangle \propto \langle \mathbf{b} | \mathcal{C} | \mathbf{a} \rangle. \quad (32)$$

On the other hand, it was shown by Knill, Laflamme and Milburn (KLM) [34] that it is possible to implement any unitary transformation using linear optical elements, single-photon sources and single-photon detectors. The simplest, nonadaptive KLM scheme uses single photons and passive linear optical elements; implementing multi-qubit gates is achieved using auxiliary helper photons. It was shown that multi-qubit gates can only be performed probabilistically in that model, and the best known CZ gate implementation succeeds with probability  $2/27$  [40]. The implementation of the gate-based circuit  $\mathcal{C}$  can be done directly using this scheme.

From either implementation, we can estimate the probability of interest by sampling  $N$  times from the output distribution of the linear optical device and outputting the ratio  $\frac{N_{post}}{N}$  where  $N_{post}$  is the number of times the post-selection condition is satisfied.

In this section, we benchmark our method against the nonadaptive KLM scheme [34] on the task of estimating the zero-zero probability of uniformly random  $q$ -qubit IQP circuits with diagonal gates  $\{Z, CZ, CCZ\}$ . We first compare the amount of samples required to get an estimation  $\varepsilon$ -close from the true zero-zero probability, then give figures on the amount of single photons needed to perform that task. We denote by  $\mathcal{I}_q$  the set of all  $q$ -qubit IQP circuits whose diagonal part is build upon the set  $\{Z, CZ, CCZ\}$ , so that  $|\mathcal{I}_q| = 2^{\binom{q}{3} + \binom{q}{2} + q}$  [30].

## B.1 Post-selection rate

In a physical experiment, the number of samples  $N$  is finite and this induces a statistical error in the estimation of the zero-zero probability. To give bounds on that error, we use standard statistical inequality [41], which states that, assuming  $X_1, \dots, X_N$  are  $N$  i.i.d. random variables of expectation value  $\mu := \mathbb{E}[X_i]$  such that  $a \leq X_i \leq b$  for all  $i = 1, \dots, N$ , then

$$\Pr \left[ \left| \frac{1}{N} \sum_{i=1}^N X_i - \mu \right| \geq \varepsilon \right] \leq \delta = 2e^{-\frac{2N\varepsilon^2}{(b-a)^2}}. \quad (33)$$

for any  $0 < \varepsilon < 1$ . For simplicity, assume  $a = b = 1$ . If  $N$  is fixed, the inequality can be used to bound the accuracy  $\varepsilon$  of the estimate for a confidence parameter  $\delta$ , where  $\varepsilon$  reads

$$\varepsilon \leq \sqrt{\frac{1}{2N} \log \frac{2}{\delta}}. \quad (34)$$

In order to apply Hoeffding's inequality to the two schemes, they must be expressed in terms of the sum of i.i.d. random variables whose expectation values – hereafter denoted  $\mu_{\mathcal{G}}$  and  $\mu_{\text{KLM}}$  for the graph encoding and KLM technique – are known. While sampling the photonic device, one has access to two quantities:  $N$ , the total number of samples, and  $N_{post}$ , the number of *post-selected* samples – for the appropriate definition of a post-selected sample. Therefore, Hoeffding's inequality can be straightforwardly applied using the observed mean value  $\frac{N_{post}}{N}$ . Depending on the scheme implemented (the graph encoding or KLM) on the photonic devices that is sampled, we denote  $N^{\mathcal{G}}$  or  $N^{\text{KLM}}$  the total number of samples and  $N_{post}^{\mathcal{G}}$  or  $N_{post}^{\text{KLM}}$  the number of post-selected samples.

### B.1.1 Post-selection for the graph-encoding technique.

Given a  $q$ -qubit IQP circuit  $\mathcal{C} \in \mathcal{I}_q$ , an estimate  $\mathcal{E}(|\text{Per}(\mathcal{G}_{\mathcal{C}})|^2)$  of the squared absolute value of the graph's permanent is obtained by sampling the output distribution induced by the  $2M \times 2M$  unitary in which  $\mathcal{G}_{\mathcal{C}}$  is embedded [17], so that

$$\mathcal{E}(|\text{Per}(\mathcal{G}_{\mathcal{C}})|^2) = \|\mathcal{G}_{\mathcal{C}}\|_2^{2M} \frac{N_{post}^{\mathcal{G}}}{N^{\mathcal{G}}}, \quad (35)$$

where  $N_{post}^{\mathcal{G}}$  is the number of samples with 1 photon in each of the  $M$  first modes. One is henceforth interested in the scaling of the ratio  $\frac{N_{post}^{\mathcal{G}}}{N^{\mathcal{G}}}$ , and in particular at what pace. The estimate we obtain from Equation (35) is ultimately written

$$\mathcal{E}(|\text{Per}(\mathcal{G}_{\mathcal{C}})|^2) = |\text{Per}(\mathcal{G}_{\mathcal{C}})|^2 \pm \delta(N^{\mathcal{G}}), \quad (36)$$

where  $\delta(N^{\mathcal{G}})$  is such that

$$\lim_{N^{\mathcal{G}} \rightarrow +\infty} \delta(N^{\mathcal{G}}) = 0. \quad (37)$$

First, we shall prove the following Lemma 1, which gives a constant upper bound on the largest singular value of  $\mathcal{G}_{\mathcal{C}}$ .

**Lemma 1.** *Let  $q, d \in \mathbb{N}^*$ . Let  $\mathcal{C} \in \mathcal{I}_q$  be a  $q$ -qubit IQP circuit of depth  $d$  and let  $\mathcal{G}_{\mathcal{C}}$  be its graph encoding. Then,*

$$\max\{1, \|A_i(\pi)\|_2 - 1\} \leq \|\mathcal{G}_{\mathcal{C}}\|_2 \leq \|A_i(\pi)\|_2 + 1, \quad (38)$$

for the largest  $i = 0, 1, 2$  such that  $\mathcal{C}$  contains the gate  $P_i(\pi)$ .

*Proof.* First, we show that for a block diagonal matrix  $A = \text{diag}(\{A^{(i)}\}_{i=1}^k)$ , its 2-norm is the maximum of the 2-norms of its blocks. Using the identity of Equation (26b), the singular value decomposition of  $A$  is performed individually on each block  $A^{(k)}$ , yielding  $A^{(k)} = U^{(k)}\Sigma^{(k)}V^{(k)*}$ . The singular values of  $A$  are therefore the union of the singular values of the blocks and in particular

$$\|A\|_2 = \max_i(\Sigma)_{ii} = \max_k \max_j(\Sigma^{(k)})_{jj} = \max_k \|A^{(k)}\|_2. \quad (39)$$

For clarity, we write  $A$  the adjacency matrix of  $\mathcal{G}_C$ . The upper bound is obtained by writing  $A = A_g + A_c$ , where  $A_g$  is the adjacency matrix of gadgets and  $A_c$  the adjacency matrix of *connectors*, *i.e.*, of edges corresponding the cycles encoding the variables as they connect together the gadgets. The matrix  $A_g$  is a block diagonal matrix, where the blocks are the  $A_i(\pi)$ 's, and  $A_c$  contains only 1's (and at most a single 1 per row). Observe that  $\|A_3(\pi)\|_2 > \|A_2(\pi)\|_2 > \|A_1(\pi)\|_2$ . As such, the triangle inequality gives

$$\|A_g\|_2 - \|A_c\|_2 \leq \|A\|_2 \leq \|A_g\|_2 + \|A_c\|_2. \quad (40)$$

By definition,  $A_g$  is a block diagonal matrix written  $A_g = \text{diag}(\{A_i^{(k)}(\pi)\}_{k=1}^n)$ , with  $n$  the number of gates in  $\mathcal{C}$ . From Equation (39),  $\|A_g\|_2 = \|A_i(\pi)\|_2$  with the largest  $i$  such that  $\mathcal{C}$  contains the gate  $P_i(\pi)$ . The matrix  $A_c$  is, by construction and up to rows/columns of zeros, a permutation of the identity matrix. Thus  $A_c$  is similar to a diagonal matrix with 0s and 1s (and it's not the null matrix) hence  $\|A_c\|_2 = 1$ . The max of the left-hand side of Equation (38) is obtained by observing that if  $\mathcal{C}$  contains no gate, then  $A$ , the adjacency matrix of  $\mathcal{G}_C$  is the identity and therefore  $\|A\|_2 = 1$ .  $\square$

The numerical values of for  $\|A_i(\pi)\|_2$  are – rounded to two decimal places – 1, 1.73, and 3.53 for  $i = 0, 1, 2$  respectively. Hence, in all generality,  $1 \leq \|\mathcal{G}_C\|_2 \leq 4.53$  for all  $\mathcal{C}$ . This result utterly aborts the hope for efficient classical strong simulation raised at the end of [13] since the norm of the adjacency matrix is lower bounded by 1 which prevents the use of Gurvit's algorithm. In practice, the numerical results suggest that  $\|\mathcal{G}_C\|_2$  grows rather slowly with respect to  $q$ , see Figure 12 and in particular it seems Equation (38) is not tight.

At first sight of Equation (35), one could argue that the singular values of the adjacency matrix can be lowered by considering the rescaled version  $\frac{1}{2^{\frac{q}{M}}}\mathcal{G}_C$ . This way,

$$\frac{1}{2^q} \text{Per}(\mathcal{G}_C) = \text{Per}\left(\frac{1}{2^{\frac{q}{M}}}\mathcal{G}_C\right), \quad (41)$$

therefore its norm becomes

$$\left\|\frac{1}{2^{\frac{q}{M}}}\mathcal{G}_C\right\|_2 = \frac{1}{2^{\frac{q}{M}}}\|\mathcal{G}_C\|_2 \leq \|\mathcal{G}_C\|_2. \quad (42)$$

However,  $M = \mathcal{O}(qd)$ . Assuming the circuits are not of constant depth, then

$$\lim_{q \rightarrow \infty} \frac{1}{2^{\frac{q}{M}}} = 1, \quad (43)$$

which means both graphs will have roughly the same norm. Moreover, the finite statistics error will be the same in the two cases.

Using Equation (35) and according to the strong law of large numbers, picking a uniformly random circuit  $\mathcal{C} \in \mathcal{I}_q$  and letting  $N^{\mathcal{G}}$  going to infinity, define

$$\mu_{\mathcal{G}} := \lim_{N^{\mathcal{G}} \rightarrow \infty} \frac{N_{post}^{\mathcal{G}}}{N^{\mathcal{G}}}, \quad (44)$$

with

$$\lim_{N^{\mathcal{G}} \rightarrow \infty} \frac{N_{post}^{\mathcal{G}}}{N^{\mathcal{G}}} \frac{\|\mathcal{G}_C\|_2^{2M}}{2^{2q}} = |\langle 0^{\otimes q} | \mathcal{C} | 0^{\otimes q} \rangle|^2. \quad (45)$$

It naturally follows from Equation (35) that

$$\mathcal{E}\left(|\langle 0^{\otimes q} | \mathcal{C} | 0^{\otimes q} \rangle|^2\right) = \frac{\|\mathcal{G}_C\|_2^{2M} N_{post}^{\mathcal{G}}}{2^{2q} N^{\mathcal{G}}}. \quad (46)$$

We define the random variables  $X_1, \dots, X_N$ , such that  $X_i = \frac{1}{2^{2q}}\|\mathcal{G}_C\|_2^{2M}$  if we select the  $i$ -th sample, and  $X_i = 0$  otherwise, so that

$$\frac{1}{N^{\mathcal{G}}} \sum_{i=1}^{N^{\mathcal{G}}} X_i = \mathcal{E}\left(|\langle 0^{\otimes q} | \mathcal{C} | 0^{\otimes q} \rangle|^2\right). \quad (47)$$

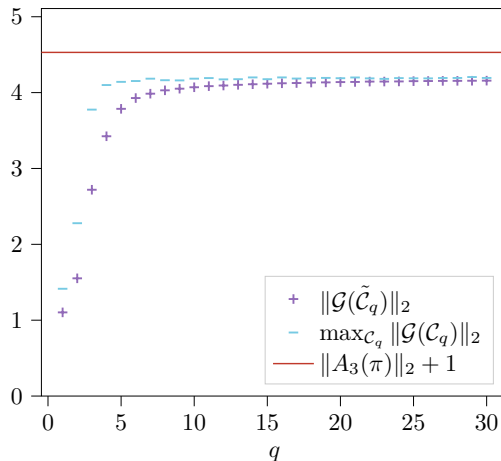


Figure 12: For each  $1 \leq q \leq 30$ , we computed the spectral norm of 5000 graphs encoding the zero-zero amplitude of randomly chosen *square* IQP-1 circuits (of depth  $d = q$ ). For each  $q$ ,  $\|\mathcal{G}(\tilde{\mathcal{C}}_q)\|_2$  is the sample average of the spectral norm, the horizontal bar show the maximum value of  $\|\mathcal{G}(\mathcal{C}_q)\|_2$  observed. All are indeed below the line  $y = 4.53$  according to [Lemma 1](#).

Accordingly, Hoeffding's inequality states that, defining

$$\varepsilon'_G := \frac{\|\mathcal{G}_C\|_2^{2M}}{2^{2q}} \varepsilon_G, \quad (48)$$

the probability that the estimate of the zero-zero probability of a circuit  $\mathcal{C}$  deviates from its actual value is

$$\Pr \left[ \left| \frac{1}{N^G} \sum_{i=1}^{N^G} X_i - |\langle 0^{\otimes q} | \mathcal{C} | 0^{\otimes q} \rangle|^2 \right| \geq \varepsilon'_G \right] \leq 2e^{-2N^G \varepsilon_G^2}. \quad (49)$$

### B.1.2 Post-selection for the KLM scheme.

In the same fashion, we can estimate the sampling accuracy of the implementation of  $\mathcal{C}$  using the KLM scheme. Let  $p_{s,\mathcal{C}} := p_{s,z}^{\#(Z)} p_{s,CZ}^{\#(CZ)} p_{s,CCZ}^{\#(CCZ)}$  be the probability that all the gates of the circuit  $\mathcal{C}$  succeed. We have

$$\mu_{\text{KLM}} := \lim_{N^{\text{KLM}} \rightarrow \infty} \frac{N_{\text{post}}^{\text{KLM}}}{N^{\text{KLM}}} = |\langle 0^{\otimes q} | \mathcal{C} | 0^{\otimes q} \rangle|^2 p_{s,\mathcal{C}}, \quad (50)$$

where, in this case,  $N_{\text{post}}^{\text{KLM}}$  is the number of samples with zeros in all the  $q$  logical qubits and with exactly one photon in each supplementary physical mode. For on-chip linear optical computation, it is convenient to consider the dual-rail encoding of the qubits. The major downside of linear optical quantum computation is the intrinsically probabilistic nature of multi-qubit operations, which results in an exponential drop of the success probability of the computation. Indeed  $p_{s,z} = 1$  as a phase is applied using a single phase shifter. We consider the Knill heralded CZ gate of [40], which succeeds with probability  $p_{s,CZ} := \frac{2}{27}$ . It requires two additional modes, each filled with a single photon. The gate is applied successfully if and only if one photon is measured at the output of each ancillary mode. A post-selected CZ gate, such as [42], has a better success probability but necessitates to post-select on having a precise pattern in the output modes which prevent the composition of several post-selected gates. Also, note that already in [34] was proposed a technique to perform near-deterministic CZ gates by utilizing large and highly entangled ancillary states and performing state teleportation, but the creation of such resource states is far beyond the reach of near-term hardware. As the induced resource overhead is nontrivial, we consider access to merely ancillary single photons. The CCZ gate can be performed using 6 CZ gates [43]. The success probability of the CCZ gate in linear optics is therefore  $p_{s,CCZ} := \left(\frac{2}{27}\right)^6$ . It has been shown in previous work that  $n$ -qubit Toffoli gates require at least  $2n$  CNOT gates when implemented without ancillary qubits [44]. Similarly, more resource-efficient Toffoli gates have been proposed, at a cost of more involved structures such as qudits [45] or cross-Kerr nonlinearity [46], but we will restrict ourselves to the standard Toffoli/CCZ implementation. Consequently, the success probability of the circuit  $\mathcal{C}$ , *i.e.*, the probability that all heralded modes are filled with exactly one photon, is

$$p_{s,\mathcal{C}} = \left(\frac{2}{27}\right)^{\#(CZ)+6\#(CCZ)}. \quad (51)$$

Define the random variables  $Y_1, \dots, Y_N$ , such that  $Y_i = 1$  if the  $i$ -th sample is post-selected, and  $Y_i = 0$  otherwise. According to Equation (50), finite experiments yield an estimate

$$\frac{1}{N^{\text{KLM}}} \sum_{i=1}^{N^{\text{KLM}}} Y_i = \mathcal{E} \left( |\langle 0^{\otimes q} | \mathcal{C} | 0^{\otimes q} \rangle|^2 p_{s,\mathcal{C}} \right). \quad (52)$$

Since  $p_{s,\mathcal{C}}$  is known for a given circuit  $\mathcal{C}$  (or at least computable in poly-time), the estimation of the zero-zero probability of a circuit  $\mathcal{C}$  one obtains from sampling the photonic device can be written

$$\mathcal{E} \left( |\langle 0^{\otimes q} | \mathcal{C} | 0^{\otimes q} \rangle|^2 \right) = \frac{1}{p_{s,\mathcal{C}}} \frac{N_{\text{post}}^{\text{KLM}}}{N^{\text{KLM}}}. \quad (53)$$

As in the previous subsection, we use the rescaled random variables  $Z_i = \frac{1}{p_{s,\mathcal{C}}} Y_i$  to build the estimate. Similarly to Equation (48), define

$$\varepsilon'_{\text{KLM}} := \frac{\varepsilon_{\text{KLM}}}{p_{s,\mathcal{C}}}, \quad (54)$$

and the error in the desired estimate is given by Hoeffding's inequality to be

$$\Pr \left[ \left| \frac{1}{N^{\text{KLM}}} \sum_{i=1}^{N^{\text{KLM}}} Z_i - |\langle 0^{\otimes q} | \mathcal{C} | 0^{\otimes q} \rangle|^2 \right| \geq \varepsilon'_{\text{KLM}} \right] \leq 2e^{-2N^{\text{KLM}} \varepsilon_{\text{KLM}}^2}. \quad (55)$$

To connect the two results, we shall prove the following Lemma 2.

**Lemma 2.** *Let  $q \in \mathbb{N}$ . Let  $\mathcal{I}_q$  be the set of  $q$ -qubit IQP circuits whose diagonal gates are drawn at random from the set  $\{Z, CZ, CCZ\}$ . Fix some desired accuracy  $\varepsilon_0$  and confidence  $\delta$ . Let  $N^{\mathcal{G}^*}, N^{\text{KLM}^*} \in \mathbb{N}$  be the number of samples needed to achieve an estimate  $\varepsilon_0$  close from the true probability with probability  $1 - \delta$  using the graph encoding technique and the KLM scheme respectively. Then, there is a function  $\alpha : \mathcal{I}_q \rightarrow \mathbb{R}$  of the number of gates and qubits of  $\mathcal{C}$ , such that*

$$N^{\mathcal{G}^*} = \alpha(\mathcal{C}) N^{\text{KLM}^*}. \quad (56)$$

*Proof.* We applied Hoeffding's inequality to the two sampling strategies in Equations (49) and (55) to derive the number of samples required to estimate of the zero-zero probability of a given circuit to particular accuracy  $\varepsilon'_{\mathcal{G}}$  and  $\varepsilon'_{\text{KLM}}$ . We write, thanks to Equation (34),

$$\varepsilon_{\mathcal{G}} = \sqrt{\frac{1}{2N^{\mathcal{G}}} \log \frac{2}{\delta}}, \quad (57)$$

and

$$\varepsilon_{\text{KLM}} = \sqrt{\frac{1}{2N^{\text{KLM}}} \log \frac{2}{\delta}}. \quad (58)$$

Ultimately, one wants to find which of the two techniques requires the least number of samples to achieve a given accuracy  $\varepsilon_0$  with probability  $1 - \delta$ . Precisely, this means finding values of  $N^{\mathcal{G}^*}$  and  $N^{\text{KLM}^*}$  such that

$$\varepsilon_0 = \varepsilon'_{\mathcal{G}} = \varepsilon'_{\text{KLM}}. \quad (59)$$

Plugging Equations (57) and (58) into the previous equation yields

$$\frac{\|\mathcal{G}_{\mathcal{C}}\|_2^{2M}}{2^{2q}} \sqrt{\frac{1}{2N^{\mathcal{G}^*}} \log \frac{2}{\delta}} = \frac{1}{p_{s,\mathcal{C}}} \sqrt{\frac{1}{2N^{\text{KLM}^*}} \log \frac{2}{\delta}}. \quad (60)$$

where we recall that

$$M = q + \#(P_0(\theta)) + 3\#(P_1(\theta)) + 5\#(P_2(\theta)) \quad (61)$$

from Proposition 2 and

$$p_{s,\mathcal{C}} = \left( \frac{2}{27} \right)^{\#(CZ) + 6\#(CCZ)}. \quad (62)$$

Then Equation (60) simplifies to

$$N^{\mathcal{G}^*} = \frac{p_{s,\mathcal{C}}^2 \cdot \|\mathcal{G}_{\mathcal{C}}\|_2^{4M}}{2^{4q}} N^{\text{KLM}^*}. \quad (63)$$

Hence, define

$$\alpha(\mathcal{C}) := \frac{p_{s,\mathcal{C}}^2 \cdot \|\mathcal{G}_{\mathcal{C}}\|_2^{4M}}{2^{4q}} \quad (64)$$

and the proof is complete.  $\square$



The natural next step is to investigate the class of circuits  $\mathcal{C}$  for which  $\alpha(\mathcal{C}) < 1$  implying that the graph encoding is more efficient to estimate a given zero-zero probability than the KLM scheme with respect to the number of samples requires. Pursuing this direction we have the following [Lemma 3](#).

**Lemma 3.** *Let  $\mathcal{C} \in \mathcal{I}_q$  be a  $q$ -qubit IQP circuit, and let  $\alpha : \mathcal{I}_q \rightarrow \mathbb{R}$  as per [Lemma 2](#). Recall that  $\#(\mathcal{U})$  is defined as the number of occurrences the gates  $\mathcal{U}$  in  $\mathcal{C}$ . Then,  $\alpha(\mathcal{C}) < 1$  if and only if*

$$\#(CCZ) > \lceil 5.68\#(Z) + 12.14\#(CZ) + 3.07q \rceil. \quad (65)$$

*Proof.* We write, for the sake of conciseness,  $x$ ,  $y$  and  $z$  instead of  $\#(Z)$ ,  $\#(CZ)$  and  $\#(CCZ)$  respectively. Recall from [Lemma 2](#) that for a given circuit  $\mathcal{C}$ , writing  $\varsigma := \|\mathcal{G}_{\mathcal{C}}\|_2$  and  $p := \frac{2}{27}$

$$\alpha(\mathcal{C}) = \frac{p^{2y+12z} \varsigma^{4q+4x+12y+20z}}{2^{4q}} = \frac{\varsigma^{4q} \varsigma^{4x} (p^2 \varsigma^{12})^y (p^{12} \varsigma^{20})^z}{2^{4q}}. \quad (66)$$

From numerical calculation of the bound of [Lemma 1](#),  $\varsigma \lesssim 4.53$ . Hence, in order to give figures, we assume that  $\varsigma = 4.53$ . We use the notation  $\log_a(b)$  to denote the logarithm of  $b$  in base  $a$  and  $\ln$  denotes the natural logarithm. Recall that we change the logarithm base from  $a$  to  $c$  using the identity

$$\log_a(b) = \frac{\log_c(b)}{\log_c(a)}. \quad (67)$$

The condition  $\alpha(\mathcal{C}) < 1$  reads

$$\frac{\varsigma^{4q} \varsigma^{4x} (p^2 \varsigma^{12})^y (p^{12} \varsigma^{20})^z}{2^{4q}} < 1. \quad (68)$$

Set  $\gamma := p^{12} \varsigma^{20} < 1$ , [Equation \(68\)](#) rewrites

$$z > -\log_{\gamma} \left( \left( \frac{\varsigma}{2} \right)^{4q} \right) - \log_{\gamma} (\varsigma^{4x}) - \log_{\gamma} \left( (p^2 \varsigma^{12})^y \right). \quad (69)$$

We evaluate each term of the right-hand side of [Equation \(69\)](#) separately. First,

$$\log_{\gamma} \left( \left( \frac{\varsigma}{2} \right)^{4q} \right) = 4q \frac{\ln \varsigma - \ln 2}{\ln \gamma} \approx -3.07q. \quad (70)$$

Second,

$$\log_{\gamma} (\varsigma^{4x}) = 4x \frac{\ln \varsigma}{\ln \gamma} \approx -5.68x. \quad (71)$$

Last,

$$\log_{\gamma} \left( (p^2 \varsigma^{12})^y \right) = y \frac{2 \ln p + 12 \ln \varsigma}{\ln \gamma} \approx -12.14y. \quad (72)$$

Plugging [Equations \(70\)](#) to [\(72\)](#) into [Equation \(69\)](#) concludes the proof.  $\square$

It remains to compute the probability that, for a fixed number of qubits  $q$ , a uniformly random circuit  $\mathcal{C} \in \mathcal{I}_q$  satisfies the condition of the previous [Lemma 3](#), which summarizes [Theorem 1](#).

**Theorem 1.** *Let  $\mathcal{C}$  be a  $q$ -qubit IQP, fix  $\varepsilon > 0$  and let  $N^{\mathcal{G}}$ ,  $N^{KLM}$  the number of samples required to estimate  $\langle 0^{\otimes q} | \mathcal{C} | 0^{\otimes q} \rangle$  using the graph encoding and the nonadaptive KLM scheme respectively. Then we can write  $N^{\mathcal{G}} = \alpha(\mathcal{C}) N^{KLM}$ , and, for large enough  $q$ , we have  $\Pr [\alpha(\mathcal{C}) < 1] \approx 1$ .*

*Proof.* Let  $S_q \subset \mathcal{I}_q$  be the set of circuits  $\mathcal{C}$  such that  $\alpha(\mathcal{C}) < 1$  and  $t(x, y, q) = \lceil 5.68x + 12.14y + 3.07q \rceil$  as per [Equation \(65\)](#). We have,

$$|S_q| = \sum_{x=0}^q \sum_{y=0}^{\binom{q}{2}} \sum_{z=t(x,y,q)}^{\binom{q}{3}} \binom{q}{x} \binom{\binom{q}{2}}{y} \binom{\binom{q}{3}}{z}. \quad (73)$$

Since no closed form for the partial sum of the binomial coefficients is known, we use the following upper bound [\[47\]](#). Let  $d \leq \frac{n}{2}$ , then

$$\sum_{k=0}^d \binom{n}{k} \leq 2^{nH(d/n)}, \quad (74)$$

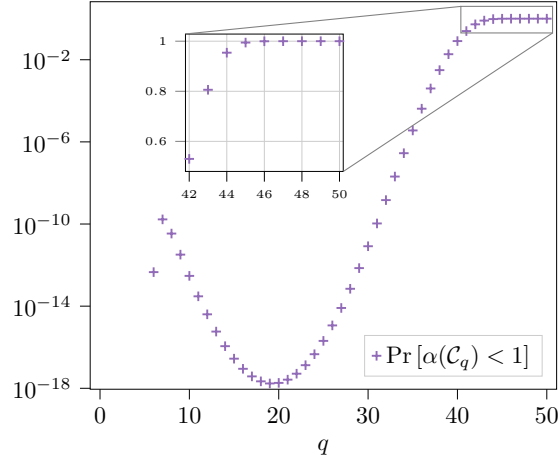


Figure 13: Log-linear plot of the numerical exact computation of the probability that a uniformly random  $q$ -qubit IQP circuit satisfies Equation (65). The  $y$ -axis of the zoomed-in plot is in linear scale.

where  $H$  is the binary entropy function defined as

$$H(x) := -x \log_2(x) - (1-x) \log_2(1-x). \quad (75)$$

Consider  $S_q^c$  the complement of  $S_q$  in  $\mathcal{I}_q$ . Then,

$$|S_q^c| = \sum_{x=0}^q \sum_{y=0}^{\binom{q}{2}} \sum_{z=0}^{t(x,y,q)-1} \binom{q}{x} \binom{\binom{q}{2}}{y} \binom{\binom{q}{3}}{z} \leq \sum_{x=0}^q \sum_{y=0}^{\binom{q}{2}} \sum_{z=0}^{t(q, \binom{q}{2}, q)-1} \binom{q}{x} \binom{\binom{q}{2}}{y} \binom{\binom{q}{3}}{z}. \quad (76)$$

In order to apply the upper bound of Equation (74), we need  $q$  such that  $t(q, \binom{q}{2}, q) - 1 \leq \frac{1}{2} \binom{q}{3}$ , *i.e.*,  $q \geq 77$ . Hence, fix  $q \geq 77$ , Equation (76) rewrites

$$|S_q^c| \leq 2^{q + \binom{q}{2} + \binom{q}{3} H\left(\frac{t(q, \binom{q}{2}, q) - 1}{\binom{q}{3}}\right)}. \quad (77)$$

Now,  $t(q, \binom{q}{2}, q)$  is a quadratic function of  $q$  while  $\binom{q}{3}$  is a cubic function of  $q$ . Hence,

$$\lim_{q \rightarrow \infty} \frac{t(q, \binom{q}{2}, q) - 1}{\binom{q}{3}} = 0, \quad (78)$$

and therefore, the binary entropy function vanishes in the limit

$$\lim_{q \rightarrow \infty} H\left(\frac{t(q, \binom{q}{2}, q) - 1}{\binom{q}{3}}\right) = 0. \quad (79)$$

Finally, using the above, we conclude the proof

$$\lim_{q \rightarrow \infty} \frac{|S_q^c|}{|\mathcal{I}_q|} = 0. \quad (80)$$

□

Said otherwise, our scheme requires less samples than nonadaptive KLM for estimating a certain probability. This is supported by Figure 13, which shows numerical computation of  $\Pr[\alpha(\mathcal{C}) < 1]$  for uniformly random  $q$ -qubit IQP circuits. The computations shown in Figure 13 were performed using the Julia programming language [26], which handles arbitrary precision arithmetic. The numerical simulation indicates that already for  $q = 44$ ,

$$\Pr[\alpha(\mathcal{C}_{44}) < 1] \approx 1. \quad (81)$$

	KLM	Graph encoding
# photons / shot	$q + 2\#(CZ) + 12\#(CCZ)$	$q + \#(Z) + 3\#(CZ) + 5\#(CCZ)$
# modes	$2q + 2\#(CZ) + 12\#(CCZ)$	$2q + 2\#(Z) + 6\#(CZ) + 10\#(CCZ)$

Table 1: Summary of the resources requirements of the KLM scheme and the graph encoding technique for estimating the zero-zero probability of a  $q$ -qubit IQP circuit with diagonal gates drawn at random from the set  $\{Z, CZ, CCZ\}$ .

Recall that we denote by  $M$  the size of  $\mathcal{G}_C$  and equivalently the number of photons per shot required to implement the probability estimation via [17]. The expected numbers of  $Z$ ,  $CZ$  and  $CCZ$  gates in a uniformly random  $q$ -qubit IQP circuit are  $\frac{1}{2}q$ ,  $\frac{1}{2}\binom{q}{2}$  and  $\frac{1}{2}\binom{q}{3}$  respectively. The expected number of photons per shot required to estimate the zero-zero probability of a uniformly random  $q$ -qubit IQP circuit using the graph encoding is therefore

$$\mathbb{E}[M] = q + \frac{1}{2} \left( q + 3\binom{q}{2} + 5\binom{q}{3} \right) = \mathcal{O}(q^3). \quad (82)$$

## B.2 Single-photons needs

The Table 1 summarizes the resources requirements of the KLM scheme and the graph encoding technique for estimating the zero-zero probability of a  $q$ -qubit IQP circuit with diagonal gates drawn at random from the set  $\{Z, CZ, CCZ\}$ . An important parameter when dealing with linear optics, and in particular near term devices, is the rate of  $n$ -photon events. State-of-the-art on-chip photonic devices can produce 6 photons events at a rate of  $\sim 4\text{Hz}$  [1]. This makes the number of photons needed in the computation a critical parameter, and in particular a factor utterly more limiting than the number of modes. To this extend, the graph encoding technique is more profitable than the KLM scheme.

Let us define the two quantities  $K(\mathcal{C}) := 2\#(CZ) + 12\#(CCZ)$  and  $G(\mathcal{C}) := \#(Z) + 3\#(CZ) + 5\#(CCZ)$ , where  $\#(\mathcal{U})$  is the number of occurrences of the gate  $\mathcal{U}$  in  $\mathcal{C}$ .  $K(\mathcal{C})$  and  $G(\mathcal{C})$  quantify the number of photons per shot (up to  $q$ ) required to estimate the zero-zero probability of the  $q$ -qubit IQP circuits associated  $\mathcal{C}$  using the KLM scheme and the graph encoding technique respectively. If the photon coincidence rate is the limiting factor of the computation, then the graph encoding is more suitable whenever  $G(\mathcal{C}) < K(\mathcal{C})$ , that is, whenever  $\#(Z) + \#(CZ) < 7\#(CCZ)$ . Conversely, KLM is more profitable than the graph encoding technique as soon as  $7\#(CCZ) < \#(Z) + \#(CZ)$ . The factor 7 depends on the CCZ implementation we chose to compare with, and might not be minimal. To that extend, we show that even if were the case that the KLM implementation becomes more advantageous when  $\#(CCZ) < \#(Z) + \#(CZ)$ , the fraction of such IQP circuits is negligible compared to the total number of IQP circuits.

The point of this short section is the following Theorem 2.

**Theorem 2.** *Let  $P_q$  be the set of  $q$ -qubit IQP circuits for which the estimation of the zero-zero probability via the graph encoding technique requires fewer photons per shot. Then,*

$$\lim_{q \rightarrow \infty} \frac{|P_q|}{|\mathcal{I}_q|} = 1. \quad (83)$$

*Proof.* The proof follows the lines of that of Theorem 1. Let  $P_q \subset \mathcal{C}_q$  be the set of  $q$ -qubit IQP circuits such that  $\#(CCZ) > \#(Z) + \#(CZ)$  and let  $P_q^c \subset \mathcal{C}_q$  be the complement of  $P_q$  in  $\mathcal{I}_q$ , that is, the set of  $q$ -qubit IQP circuits for which the estimation of the zero-zero probability via the graph encoding technique requires more photons per shot. Precisely,  $P_q^c$  is the set of  $q$ -qubit IQP circuits such that  $\#(CCZ) < \#(Z) + \#(CZ)$ , whose cardinality is given by

$$|P_q^c| = \sum_{x=0}^q \sum_{y=0}^{\binom{q}{2}} \sum_{z=0}^{x+y-1} \binom{q}{x} \binom{\binom{q}{2}}{y} \binom{\binom{q}{3}}{z} \leq \sum_{x=0}^q \sum_{y=0}^{\binom{q}{2}} \sum_{z=0}^{\binom{q}{2}+q} \binom{q}{x} \binom{\binom{q}{2}}{y} \binom{\binom{q}{3}}{z}. \quad (84)$$

To use the upper bound of Equation (74), we need to find  $q$  such that  $\binom{q}{2} + q \leq \frac{1}{2}\binom{q}{3}$ , that is,  $q \geq 10$ . Hence,

$$|P_q^c| \leq 2^{q + \binom{q}{2} + H\left(\frac{q + \binom{q}{2}}{\binom{q}{3}}\right)\binom{q}{3}}, \quad (85)$$

and as such, as  $q$  grows, the probability that a uniformly random  $q$ -qubit IQP circuit is such that  $\#(CCZ) < \#(Z) + \#(CZ)$  is given by

$$\lim_{q \rightarrow \infty} \frac{|P_q^c|}{|\mathcal{I}_q|} \leq \lim_{q \rightarrow \infty} \frac{2^{q + \binom{q}{2} + H\left(\frac{q + \binom{q}{2}}{\binom{q}{3}}\right) \binom{q}{3}}}{2^{q + \binom{q}{2} + \binom{q}{3}}} = 0. \quad (86)$$

□

In other words,  $\#(CCZ) > \#(Z) + \#(CZ)$  almost surely for large enough  $q$  and the graph encoding technique requires fewer photons per shot.